EVALUATION OF HOT SURFACE IGNITION DEVICE PERFORMANCE WITH HIGH-PRESSURE KEROSENE FUEL SPRAYS

BY

AUSTEN MOTILY

THESIS

Submitted in partial fulfillment of the requirements
for the degree of Master of Science in Mechanical Engineering
in the Graduate College of the
University of Illinois at Urbana-Champaign, 2020

Urbana, Illinois

Advisor:

Professor Tonghun Lee

ABSTRACT

Among the range of commercially feasible propulsion systems, compression ignition (CI) engines present many advantages for light-duty vehicle operation. In particular, CI engines remain an optimal choice for unmanned aerial vehicles (UAVs) designed to operate at moderate flight speeds. However, one of the primary limitations of CI engines is that they require well-characterized, highly-reactive diesel fuel to operate properly. As the United States Department of Defense implements the single fuel concept and with global efforts to develop alternatively derived fuels, it is paramount that modern CI engines have the capability to perform with a diverse variety of fuel types. At its core, this challenge can be framed as an ignition problem, where low reactivity fuels and extreme operating conditions result in long ignition delays, engine misfires, and power loss. It is for this reason that novel ignition devices be developed to support reliable CI engine operation. Hot surface energy addition devices are a promising technology to improve ignition behavior, but the mechanisms by which the heating element supports the ignition process are not well understood.

This study evaluates the performance and limitations of commercial off-the-shelf (COTS) heating elements in functioning as continuous-use ignition devices for kerosene-fueled CI engines. Furthermore, it examines the interaction between a single high-pressure fuel spray with a hot surface device in order to identify the most important parameters for optimizing ignition behavior. Results of these experiments demonstrate that existing heating elements can accelerate the ignition process for fuels with a wide range of reactivities, assuming a sufficient surface temperature can be achieved. Reaching these temperatures in an engine environment and maintaining these temperatures for long periods of operation, with acceptable heating element durability, will be the primary challenges in developing next-generation ignition systems.

ACKNOWLEDGMENTS

A great number of people have been involved, both directly and indirectly, in making this work possible. I can think of nobody more influential in my life than my parents, who fostered my curiosity from an early age and have supported my pursuits in higher education. As my first true teachers, they have cultivated an indelible sense of creativity and focus that shapes my mindset to this day. I am fortunate to have an affectionate extended family, of which my numerous aunts, uncles, cousins, and grandma have remained such a positive force in my life. It would be remiss of me to fail to mention the various teachers and professors who have guided me throughout my educational career, both technical and otherwise, and continue to invest their time with genuine interest in their students.

On the technical side, I would like to thank my advisor, Prof. Tonghun Lee, for providing me the opportunity to conduct academic research. His dedication to maintaining world-class facilities and equipment has allowed me to pursue high-quality scientific results and has motivated me to take on challenging projects. I am grateful for my fellow lab members, who have assisted with experiments and established a friendly work environment. Finally, I would like to thank the Combat Capabilities Development Command Army Research Laboratory, Vehicle Technology Directorate and the numerous scientists and managers that I have collaborated with for their contributions to this work and their support in pursuing meaningful research with practical outcomes.

Partial results of the presented work have been published in AIAA Paper 2020-2280, 2020 or submitted to the Proceedings of the Combustion Institute, 2020.

TABLE OF CONTENTS

CHAPTER 1: INTRODUCTION

1.1 Motivation

The United States Army supports operation of a wide variety of land and air vehicles in various locations around the world. For these vehicles, which often operate in hostile environments, dependability is crucial to achieving mission success. Due to their fuel efficiency and reliability, direct injection compression ignition (CI) engines are the propulsion system of choice for a large portion of U.S. Army vehicles. Among the most extreme applications of CI engines is unmanned aerial vehicle (UAV) propulsion, where harsh operating conditions at increased altitude and long periods of runtime push engine technology to its limits.

Compounding the issues of CI engine operability is the variation in fuel composition and reactivity encountered in the field. The Army requires different fuels for the two primary propulsion systems: diesel fuel for CI engines and jet fuel for gas turbine engines. However, away from the base of operations, sourcing multiple fuels is difficult and can hinder mission success. The clear solution to this problem is to reduce the burden on the supply chain by only sourcing a single fuel. It is for this reason that the United States Department of Defense has adopted the single fuel concept where all vehicles should use a common fuel while deployed. Furthermore, in the event of a supply chain cut off, the Army can maintain operational flexibility by using whatever fuel is available, although it may not be well-characterized and may exhibit low reactivity. However, current CI engines are only designed to operate with standard diesel fuel and can encounter several complications when powered by lower-reactivity kerosene-based jet fuel. With these challenges in mind, the army has established a program to develop multi-fuel capable engines that can function with a wide variety of fuel types.

The issues associated with extreme operating conditions and the potential for encountering low quality fuels combine to make development of a multi-fuel capable engine challenging. At reduced top dead center (TDC) pressures and temperatures, chemical reaction rates are slowed and operation with low reactivity fuels can result in extended ignition delays, misfires, and system power loss. Additionally, mismanagement of the engine control scheme can lead to large pressure rise rates, knocking, and even mechanical damage. From an engineering perspective, these problems arise from variability in cycle-to-cycle ignition behavior and are a direct result of poor autoignition performance. In order to improve ignition behavior, novel ignition enhancement methods must be developed to support reliable operation of Army CI engines.

1.2 Methods for Energetically Enhanced Ignition

There are several devices and schemes that can be implemented to promote CI engine ignition performance. These methods utilize various technologies to add energy to the combustion system in an attempt to accelerate the ignition process. The strategies can be broadly categorized as methods involving exhaust gas recirculation (EGR), fuel heating, or air heating.

The first scheme to consider is that of external EGR, where a portion of the exhaust is re-routed externally back into the combustion chamber. EGR is typically used to reduce emissions rather than as an ignition enhancement method. As shown in Figure 1, external EGR requires additional infrastructure to be implemented in the propulsion system, and may not be possible for weight or volume constrained vehicles [1].

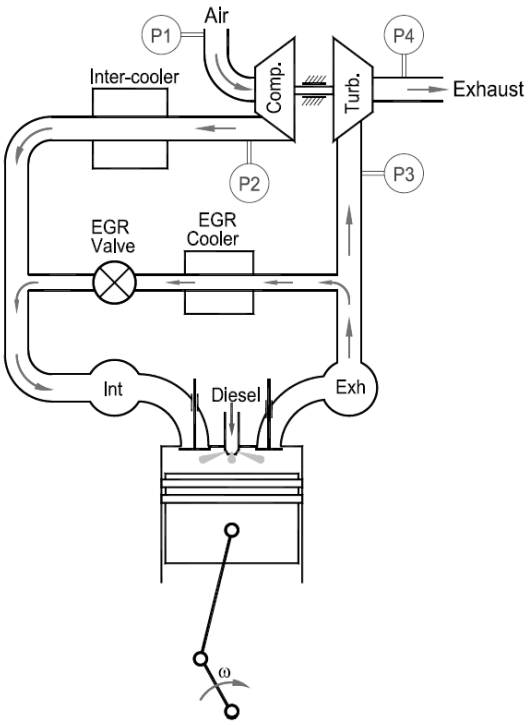

Figure 1. Diagram of high-pressure-loop EGR [1]

Some EGR studies have been conducted with lower quality fuels, but results indicate that EGR tends to exacerbate differences in reactivity rather than support multi-fuel operation [2].

Another option to consider is that of internal EGR, where variable valve timing is leveraged as an actuator and used to regulate residual gas fraction. Combustion stability has been demonstrated successfully in homogeneous charge compression ignition (HCCI) engines, but requires parameter tuning and will exhibit reduced stability limits at increased altitude when using low quality fuels [3]. Furthermore, this method inherently requires a cam phasing mechanism, which makes it impractical for retrofitting some existing Army vehicles. For both EGR schemes, utilizing burned gases as part of the working fluid reduces the oxygen content and can be detrimental to ignition performance if not controlled correctly. Relying on the ignition of previous cycles can be problematic for these control schemes, especially when dealing with high-variability conditions at the end of the operational envelope.

Fuel preheating is another method that could be used to assist ignition performance. In the literature, it has typically been implemented to reduce the viscosity of exotic fuels such as vegetable oils and improve operation with standard diesel injectors [4-5]. Slight efficiency gains have been demonstrated for moderate increases in fuel temperature, but to implement this strategy in an actual vehicle, a heating system would need to be designed and installed.

One of the more common energy addition methods is external air heating. This method utilizes a heat exchanger on the intake to transfer heat to the working fluid and achieve higher temperatures when the air is compressed. Previous studies have employed this strategy in dual-fuel engines, out of a necessity to vaporize the fuel that is carried with the heated intake air. However, increasing the inlet temperature typically reduces volumetric efficiency, and the required heat exchanger presents weight and volume challenges for vehicle design.

The last option for ignition assisting strategies is internal air heating. For this method, air is heated inside the combustion chamber by a resistive heating element commonly known as a glow plug. Figure 2 shows a cross section of a direct injection CI engine with an activated heating element [6].

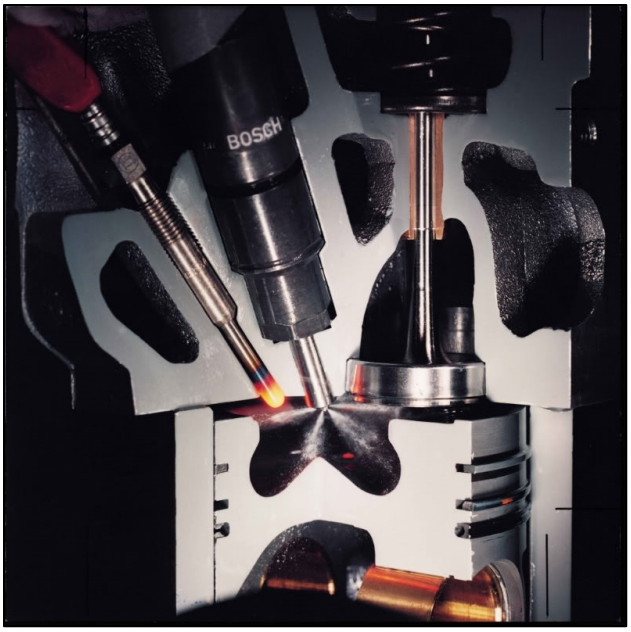

Figure 2. Cross section of direct injection CI engine combustion chamber with activated metal heating element [6]

These devices are typically only used to improve startup performance of CI engines in cold-weather conditions, but there exists significant literature demonstrating applications where these "hot surface energy addition" devices can support low-quality fuel operation. The primary concern with this strategy is durability, as temperatures above 1000 K are necessary to support reliable ignition performance.

A large benefit of this method is that an improved hot surface ignition device design can replace existing heating elements without significant modifications to existing Army vehicles. Due to relative success demonstrated in the literature and practical installation requirements, this method is selected as the most promising technology for enabling multi-fuel capable engine operation. Other energy addition methods can be considered, such as sparks, corona discharges, or plasma assisted combustion strategies, however heating elements afford the most promising near-term performance that can be easily adopted with existing engine infrastructure.

1.3 Hot Surface Ignition Devices

Resistive heating elements have been utilized to enhance ignition of fuel sprays since the early 1900s [7]. Originally designed to assist compression ignition engines during startup, the performance and design of these devices has improved significantly since their inception. The first iterations of these devices utilized exposed metal heating elements, as demonstrated in Figure 3.

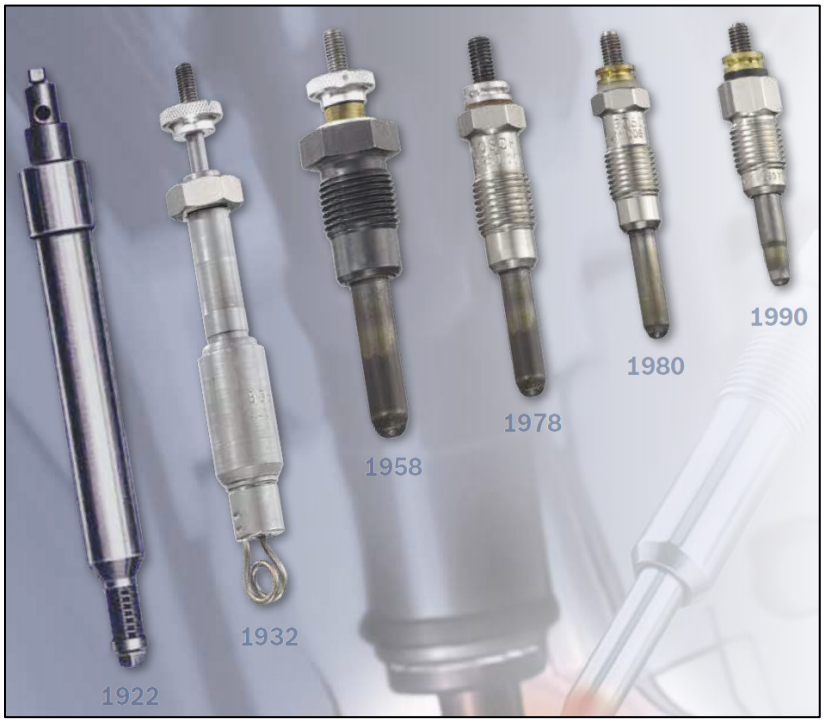

Figure 3. Evolution of heating element technology in the 20th century [8]

Designs shifted to sheathed-element devices, where the internal conducting structure was protected and insulated by a corrosion-resistant metal cover. Around the end of the 20th century, ceramic heating elements were being developed in order to achieve higher surface temperatures and extended lifetimes.

As significant advances in heating element durability were made, engineers began to study the feasibility of using heating elements as constant energy addition devices. Rigorous

experimental investigations began in the 1980s as researchers attempted to understand the limitations of running passenger vehicles on alternative fuels with poor autoignition behavior. Studies on methanol and ethanol-fueled diesel engines demonstrated relatively long runtimes with some limitations on device durability [9-10]. However, convective cooling of the surface limited ignition reliability, so heating element shields which partly cover the hot surface were utilized. As early as 1990, it was understood that a shield should be implemented to reduce thermal losses to the intake air [11]. This realization also suggested that energy deposition from the heating element was a local phenomenon; the hot surface energy addition device does not serve to heat the entire volume of air within the combustion chamber, but rather the air/fuel mixture in the thermal boundary layer surrounding the surface. For this reason, the term "internal air heating" is a slight misnomer and it is more appropriate to refer to the heating element simply as an ignition device.

More recently, significant experimental and computational resources have been devoted to understanding the effects of hot surface ignition on heavy-duty direct injection natural gas (DING) engine performance [12-14]. However, few studies have rigorously investigated the ignition behavior of jet fuel or other heavy fuel sprays when interacting with a heating element [15]. Previous research has identified heating element temperature and position as the primary factors affecting ignition performance [16]. Mueller and Musculus demonstrated stable operation of an engine on M100 methanol fuel when sufficient voltage was applied and an acceptable heating element orientation was achieved [17]. However, characterizing the heating element surface temperature in-engine is difficult, and only an estimate for the temperature was provided in this study.

Surface temperature is strongly affected by in-cylinder flows, and the heating element shields used to reduce convective cooling introduce additional complexity and can even hinder fuel-air mixing [18]. The combined effect of these variables on actual surface temperature is difficult to model, and no experiments have been performed to systematically evaluate the effects of temperature on hot surface assisted ignition. The rapid compression machine (RCM) used in this study allows for analyzing the ignition behavior and heating element interaction in a controlled environment and at variable surface temperature. Surface temperature is not only an important parameter for combustion stability, but plays an important role in device durability [19]. Identifying a lower bound for stable combustion is essential in prolonging device lifetime and enabling the use of heating elements as a practical method for igniting low-quality fuels.

1.4 Goals and Objectives

Hot surface energy addition devices demonstrate great potential for enabling multi-fuel capable engine operation. However, the interaction between the fuel spray and heating element must be studied in greater detail to facilitate the design of novel continuous-use ignition devices. Heat transfer that occurs from the heating element to the two-phase spray is a complex process that should be investigated to quantify energy deposition relevant to ignition. The effect of in-cylinder flows and convective cooling must be evaluated to assess how heat transfer to the bulk air can be minimized. Studying the residence time of the ignitable mixture in the vicinity of the heating element surface will allow for optimization of device geometry and temperature requirements. Assessing durability and improving device lifetime is paramount to ensuring these devices can be implemented reliably for operation with army vehicles.

With these scientific goals in mind, the present work aims to evaluate the performance of existing heating elements in order to inform the design of next-generation ignition devices. The

maximum surface temperatures and time constants of commercial off-the-shelf (COTS) heating elements are characterized in order to establish baseline performance. An RCM, shown in Figure 4, is used to evaluate the effect of heating element surface temperature on spray ignition behavior in a controlled environment.

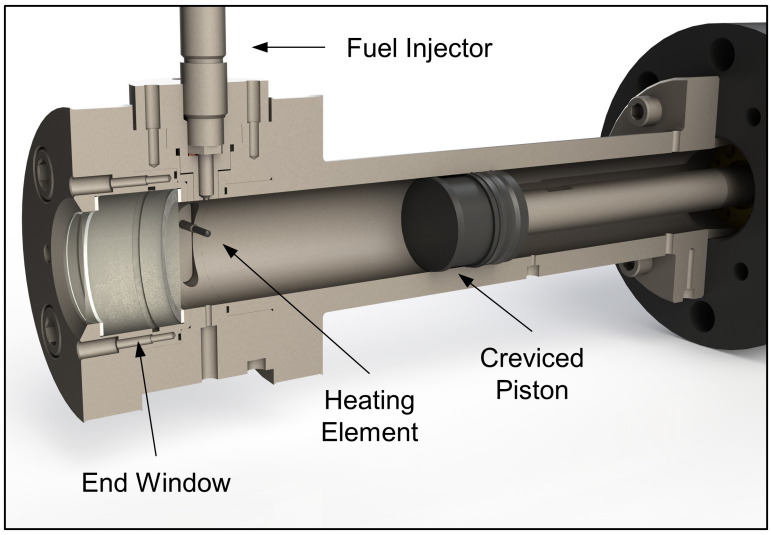

Figure 4. RCM cutaway depicting combustion cylinder, optical head, injector, and hot surface device

The present work evaluates how the relative geometry between a single fuel jet and heating element affects flame kernel formation at increased elevation operating conditions encountered by UAVs. The effects of fuel reactivity on hot surface assisted fuel spray ignition are also examined. A preliminary assessment of device durability is performed, and the results are summarized. Finally, potential avenues for future research are described and the remaining challenges for developing next-generation ignition devices are discussed.

CHAPTER 2: EXPERIMENTAL METHODS

2.1 Benchtop Experiments

Modern, commercially available hot surface ignition devices can be categorized into two main types based on the material which comprises the heating element sheath: metal or ceramic. In the automotive industry, metal heating elements are generally older technology and are limited to surface temperatures of around 1200 K. Ceramic heating elements can reach higher surface temperatures and exhibit faster startup times, but they are fragile and can be difficult to handle and install. Before studying the influence of a hot surface device on fuel spray ignition performance, it is important to accurately characterize the heating behavior of the device itself and identify performance differences between models. The first benchtop experiment presented here is designed to compare the startup performance of 8 different brands of metal heating elements, all designed for use in the Alpha Romeo 156 1.9 JTD engine. A bare wire thermocouple is used to measure the heating element tip temperature and the data is logged with a LabVIEW data acquisition system.

Ceramic heating element performance is generally superior to heating elements fabricated from metal. A single ceramic hot surface device, the Bosch Duraspeed 0250603008, is selected for characterization based on its high advertised maximum surface temperature (1200 °C) and geometric compatibility for use with the RCM. The remainder of the present work is conducted using the Bosch 0250603008, including the spray ignition experiments and the durability assessment.

2.2 Rapid Compression Machine

The primary experimental apparatus utilized in this study is the RCM. Functionality and operation of this device has been described in several previous works, so a brief description will

be given here [20-22]. This device simulates a single compression stroke of a piston-cylinder engine and can be used to study a variety of phenomenon related to homogeneous mixture and fuel spray combustion. The RCM is a pneumatically-driven, hydraulically-stopped shaft and piston that compresses the gas within the combustion chamber to the desired conditions. The maximum compressed pressure and temperature that the RCM can achieve is about 40 bar and 900 K, respectively. Figure 5a shows the inside of the RCM cylinder with the end cap of the combustion chamber removed.

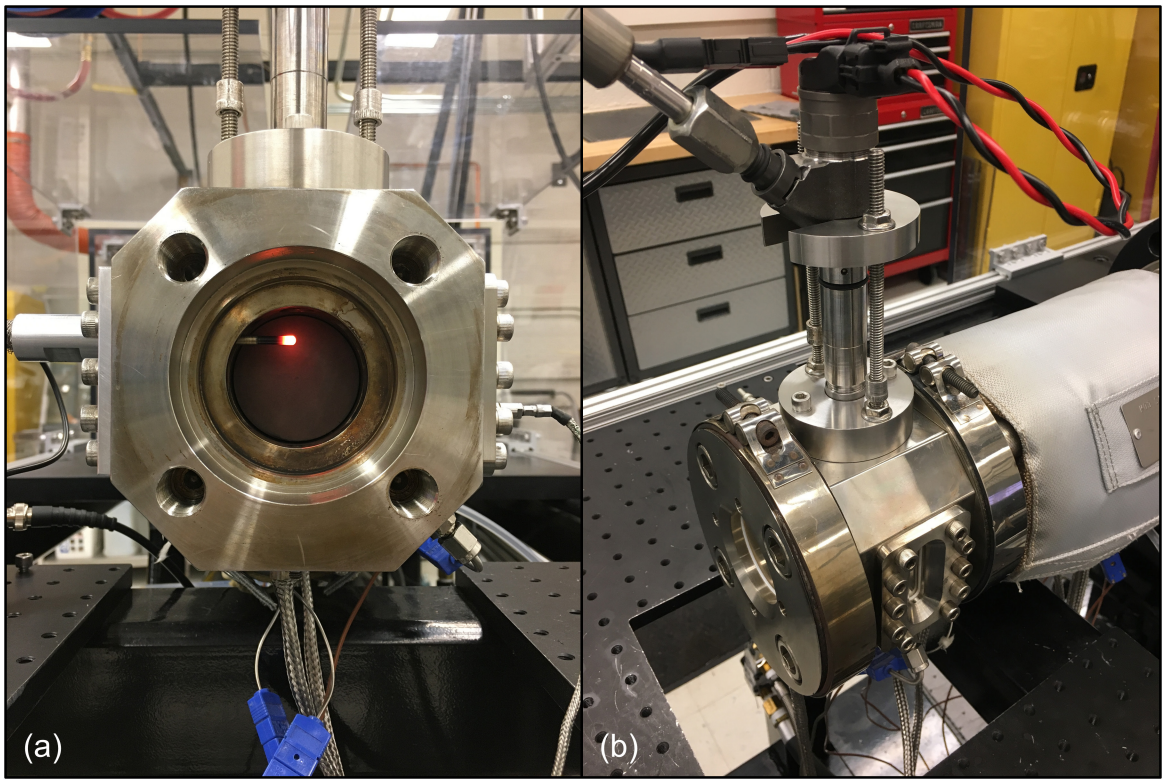

Figure 5. Activated ignition device in rapid compression machine combustion chamber (a) and mounted injector (b)

The combustion cylinder head was designed with four windows for optical access, and imaging in this study is performed through the largest window with the camera aligned along the cylinder axis. This will be referred to as the "end window." Stroke shims, compression cylinder shims, piston spacers, and the end window can all be modified to adjust the RCM compression

ratio and compressed temperature. The RCM is heated to 400 K to achieve the desired in-cylinder temperature after compression.

In contrast to previous studies with this experimental apparatus, a new optical head with rounded rectangular side windows is utilized. These windows provide geometrical flexibility and increased optical access for studying ignition systems. A hot surface ignition device is introduced into the chamber via the left side window. Mounting inserts were fabricated to fit within the window geometry while also sealing the chamber pressure. Technical drawings for the mount can be found in the Appendix. The hot surface device used for spray ignition measurements is a Bosch 0250603008 Duraspeed glow plug. It utilizes a ceramic heating element and exhibits relatively fast startup times and high steady-state surface temperatures. Insertion distance of the device into the chamber can be modified with copper spacers that also help to seal chamber pressure. The device can be seen in Figure 5a mounted in the RCM and activated with the nominal 7 V applied. The cylinder is 50.8 mm (2 in.) in diameter.

A high-speed pressure transducer (Kistler 6125C) measures pressure within the combustion chamber throughout the experiment. A dual-mode signal amplifier (Kistler 5010B) amplifies the pressure signal that is recorded with a LabView data acquisition system. The signal is sampled at 100 kHz and post-processed with a zero-phase digital Butterworth filter at a cutoff frequency of 2,000 Hz. The controlled environment after compression relies on the adiabatic core assumption, where only a small thermal boundary layer surrounding the chamber walls experiences a significant temperature gradient throughout the testing duration. The creviced piston design reduces roll-up vortices and better maintains the adiabatic core assumption for a given trial [23]. With this assumption, the temperature of the cylinder gases after compression

can be calculated from the pressure trace during post-processing. An isentropic compression process of a gas with heat capacity c_p and a gas constant R can be described with Equation (1).

$$\int_{T_0}^{T_c} \frac{c_p}{R}\frac{dT}{T} = \ln\left(\frac{P_c}{P_0}\right) \quad (1)$$

where P and T are pressure and temperature, respectively. The subscript c denotes the compressed condition while a subscript 0 indicates the initial state. Assuming isentropic compression processes from one data point of pressure to the next, this equation can be integrated numerically and with good accuracy using the thermodynamic parameters for nitrogen and oxygen prescribed by Burcat [24]. The mixture is approximated as 21% O_2 and 79% N_2 corresponding to the "dry air" compressed gas cylinder composition utilized for the experiments.

Spray Injection System

To conduct fuel spray ignition measurements, a high-pressure diesel fuel injector is introduced into the combustion chamber via the top window port and secured with a custom injector mount. The part drawings for the mount are included in the Appendix. The injector used in this study is a modified on-axis single-hole Bosch CRIN3 injector. This injector has been characterized in a high-pressure vessel with JP-8 fuel [25]. The opening time of this injector based on the injection analyzer from the study was 0.43 ms, and this value has been verified in the present study by front-illuminated 30 kHz Mie scattering images from a halogen lamp light source. Figure 5b shows the injector mounted to the top of the RCM optical head. The high-pressure fuel spray is oriented downwards into the chamber. High-pressure fuel is supplied with a pneumatically driven hydraulic pump. The fuel is distributed with a Bosch fuel rail and maintained at a pressure of 40 MPa for all trials. Injection timing is set to 100 ms after top dead center (ATDC) to minimize the effects of transient in-cylinder flows. The injection command is

sent from the data acquisition system after the pressure has stabilized at the compressed condition. A Drivven injection system receives the trigger and controls the injection duration, which is set to 1.5 ms for all trials. The heating element is inserted horizontally, located 12 mm downstream of the nozzle tip. The resulting relative geometry between the spray axis and heating element axis for this study is perpendicular. The angular orientation between these two devices in practical applications varies depending on the engine design but is generally between 90 and 120 degrees. More relevant is the insertion depth of the hot surface into the chamber. Insertion depths in an engine are generally less than 15 mm, but for this study, the nominal position utilizes a 24.9 mm insertion depth to capture proper surface/spray interaction. This results in a 0.5 mm perpendicular distance from the spray axis centerline to the heating element tip.

Heating Element Control

Heating element surface temperature is an important parameter influencing ignition behavior [26]. Due to the difficulty of measuring this value accurately in-engine during experiments, the precise effects of this variable on ignition delay have not been well characterized. This study investigates a wide range of surface temperatures by timing the compression and injection event of the RCM with the temperature rise of the surface once the nominal voltage (7 V) is applied to the device. As the device heats up, the electrical resistance increases so that the device can “self-regulate” or avoid over-heating and melting of the internal components. The temperature rise of the heating element tip in the chamber was recorded at ambient pressure with a 0.003 in. diameter butt-welded K-type thermocouple with a 0.04 s time constant. Care was taken to ensure adequate thermal contact for accurate temperature measurement. The surface temperature timing diagram is shown in Figure 6.

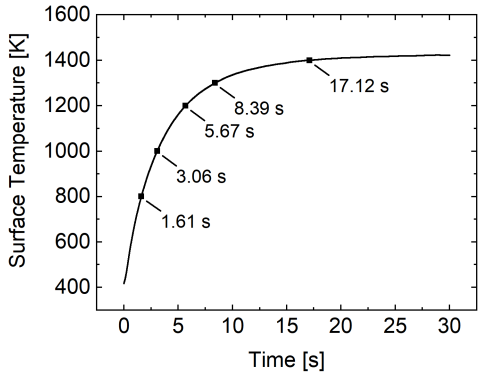

Figure 6. Bosch 0250603008 heating element tip surface temperature during startup in RCM and associated injection timing

High-Speed Imaging

A Photron SA5 camera is used to record broadband luminescence images of the flame through the RCM end window at frame rates of 10 kHz with a resolution of 896 x 848 pixels. At full resolution, (1024 x 1024 pixels) the field of view was significantly larger than the combustion cylinder region of interest, so a reduced resolution setting was used to take advantage of higher speeds. The camera was fitted with a Cerco 100-mm f/2.8 UV-VIS lens. For spray visualization in non-reactive trials, a 150 W dual halogen lamp is used to illuminate the inside of the combustion chamber. A reduced resolution is used to image the inert spray at a framerate of 30 kHz. A diagram of the experimental setup along with the supporting infrastructure can be seen in Figure 7.

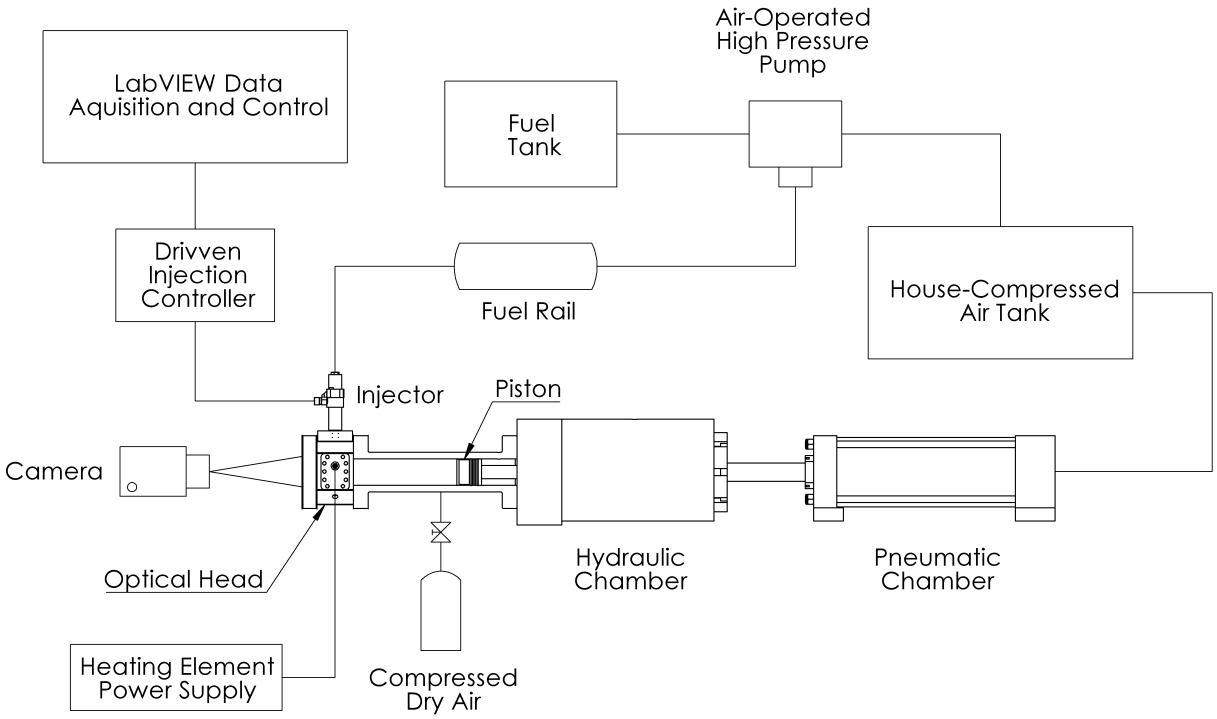

Figure 7. Experimental diagram of RCM and auxiliary infrastructure

Cetane Number Fuels

One of the key pursuits to enabling multi-fuel capable CI engines is understanding the effect of the hot surface device on the ignition behavior of fuels with different reactivities. Throughout operation, the engine may encounter various fuel types and low-quality fuels that hinder reliable engine operation. Low reactivity fuels are associated with long ignition delays, where it takes an extended time period (on the order of several milliseconds) for the fuel to vaporize, break down chemically, and produce a sufficient amount of exothermic reactions for positive net heat release to occur. In order to quantify fuel reactivity, the engine community has reduced this complex multivariable process into an empirical parameter known as the cetane number.

The cetane number is a measure of the autoignition performance of a fuel. There is a standardized process used to assign the value to a particular fuel, where the ignition delay is

measured in a standardized cooperative fuel research (CFR) engine at specified conditions. Performance is compared to two reference fuels and assigned a value based on a scale from isocetane at 15, which is less reactive, to cetane at 100, which has exceptional reactivity. Kerosene based fuels, of particular interest in this study, typically exhibit cetane numbers around 45, whereas standard diesel fuel is characterized by cetane numbers around 55. Figure 8 compares the cetane number of various common fuel types.

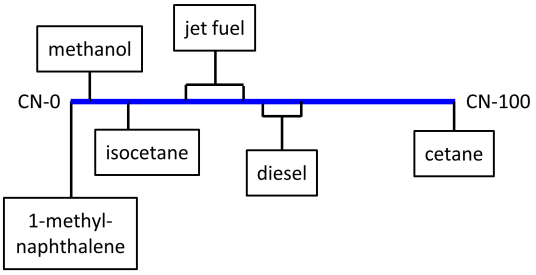

Figure 8. Cetane numbers of common fuel groups and reference fuels

One disadvantage of using the cetane number is that it includes the combined effects of physical delay (spray breakup, atomization, evaporation) and chemical delay (reaction rates). It is difficult to separate the effects of chemical kinetics from overall spray ignition behavior, so spray ignition studies targeting fuel reactivity as the sole independent variable can be difficult to conduct. To address this issue, the Army Research Laboratory has formulated Jet-A kerosene fuels with similar physical properties and variable cetane number, which will be referred to in this study as “cetane fuels.” When utilizing these fuels, performance differences can be attributed to reactivity only, which is advantageous for the present work that examines the effect of low-quality fuels on hot surface ignition behavior. Three cetane fuels are utilized in this study, with nominal cetane numbers ranging from 30 to 40 as shown in Table 1.

Table 1. F-24 and Varied Cetane Number Fuel Properties [27-28]

Fuel	Cetane Number	Molecular Weight [g/mol]	Density [g/cm^3]	Viscosity [mm^2/s]
CN 30	30.0	159.3	0.78	4.01
CN 35	35.2	156.8	0.78	3.84
CN 40	41.0	166.5	0.80	4.80
F-24	48.5	160.6	0.80	1.38*

* viscosity measured at 40 °C, CN fuels measured at -20 °C

A detailed description of the cetane fuels is provided in Ref. [27]. The autoignition behavior was adjusted by changing chemical group composition. Min et al. evaluated the autoignition performance of these fuels in the low to mid temperature regime to investigate reaction chemistry and multi-stage contributions to overall ignition delay [27]. Whether or not the unique low temperature behavior of these fuels is present in energy assisted spray ignition has yet to be explored.

RCM Experimental Parameters

There are two spray ignition experiments conducted in this study. The first set of measurements evaluates the influence of heating element position with the reference fuel F-24, a Jet-A derivative with additives utilized by the U.S. Army. The second experiment investigates the effect of fuel reactivity on ignition behavior by using varied cetane number kerosene-based fuels with similar physical properties. Both experiments study a range of heating element temperatures from 400 K to 1400 K, while the in-cylinder compressed air conditions are 800 K and 30 bar for all trials. These conditions represent an extreme-case thermodynamic state for CI engine TDC low-load operation at altitude.

For the first experiment, three different insertion depths are tested, starting with the heating element tip one millimeter past the nozzle centerline, and then pulled out in increments of 1.5 mm. For all insertion depths, experiments are conducted with surface temperatures of 400 K (no voltage), 800 K, 1000 K, 1200 K, 1300 K, and 1400 K. Where significant changes in

ignition delay are observed between these conditions, additional surface temperatures are selected. For the second experiment, the middle insertion depth is utilized, where the heating element tip is 0.5 mm from the nozzle centerline. The three cetane fuels have nominal cetane values of 30, 35, and 40. Experimental conditions and parameters for both studies are summarized in Table 2.

Table 2. Fuel Spray Ignition Experimental Parameters

Fuels	F-24, CN 30-40
Oxidizer Mixture	Air (dry)
Compressed Pressure	30 bar
Compressed Temperature	800 K
Injector Type	Bosch CRIN3
Number of Orifices	1
Orifice Diameter	147 μm
Injection Pressure	40 MPa
Injection Duration	1.5 ms
Injection Timing	100 ms ATDC
Hot Surface Device	Bosch Duraspeed
Nominal Voltage	7 V
Distance from nozzle	12 mm
Distance from spray axis	-1.0, 0.5, 2.0 mm
Surface Temperature	400-1400 K

Ignition Delay Definition

Several methods exist in the literature for calculating ignition delay based on a pressure trace of a combustion vessel. For homogeneous mixtures, the maximum slope of the pressure curve is used as a repeatable way to designate when ignition has occurred. For spray ignition however, the pressure rise due to combustion is generally smaller, and the maximum pressure rise can vary in time from trial to trial. Better methods for calculating the ignition delay exist which are relevant to liquid fuel sprays in particular. The liquid spray ignition delay can be separated into two stages, which have been characterized in an RCM [29]. The start of injection (SOI) is defined as the time when fuel first enters the cylinder. The SOI definition is important because there is a delay from the injection trigger signal to the SOI due to the time it takes the

injector to open. Once fuel is injected into the chamber and is atomized, it evaporates as heat is transferred to it by the compressed gases. The resulting decrease in gas temperature results in a slight pressure drop, which continues as more of the fuel is vaporized. At the onset of exothermic reactions, heat release causes an increase in cylinder pressure, and as ignition proceeds the pressure rises above the pressure that would be observed in a no-injection trial. The times for exothermic reactions to occur and pressure to recover beyond the no-injection case are defined as the two stages of ignition delay, and can be determined from a non-reactive trial (in nitrogen, for example) and a test without injection at the same conditions [30]. Other methods for calculating ignition delay can model heat loss and utilize the maximum heat release rate to define ignition [31]. Compared to the long ignition delays measured for low pressure and low temperature combustion studies, the short ignition delay times here result in small decreases in pressure due to heat loss to the walls. In this case, it is appropriate to define a pressure recovery ignition delay. This delay represents the time it takes for the in-cylinder pressure to recover to its initial value at the start of injection and corresponds to the definition in [29] with the adiabatic wall approximation. Figure 9 depicts the pressure drop due to vaporization and a visual representation of the method used to calculate ignition delay, with time prescribed after the start of injection (ASOI).

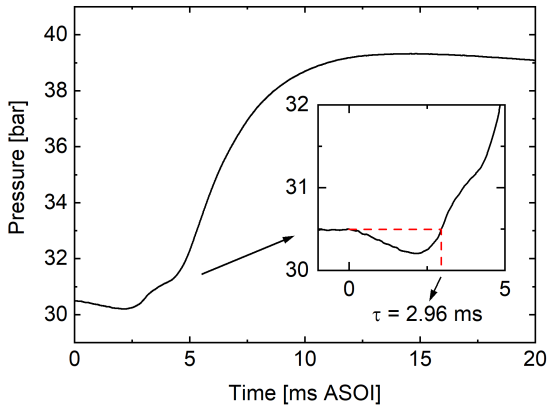

Figure 9. Pressure trace of CN 30 ignition event (solid), heating element not powered with pressure recovery ignition delay (τ) defined from the SOI to the time at which pressure recovers to the initial value (dashed)

Apparent Heat Release Rate

An additional metric that the pressure trace can provide is the apparent heat release rate (AHRR) during the ignition process. The AHRR $\frac{dQ_c}{dt}$ can be estimated from the time derivative of the pressure trace, $\frac{dp}{dt}$ using Equation (2).

$$\frac{dQ_c}{dt} = \frac{V}{\gamma - 1}\frac{dp}{dt} + \frac{dQ_{ht}}{dt} \tag{2}$$

where V is the compressed volume, γ is the specific heat ratio, assumed here to be constant (1.4) throughout the combustion process, and $\frac{dQ_{ht}}{dt}$ is the heat loss to the walls. The heat loss can be estimated with convective heat transfer correlations, or calculated from non-reactive trials without injection. A previous study with a similar RCM design demonstrated that convective cooling decays exponentially ATDC with a time constant around 20 ms [31]. Therefore, to minimize the effects of convective cooling in the heat release calculation, the injection timing used for this study is five time constants ATDC, or 100 ms. The study also demonstrated that radiative heat loss is negligible. The heat loss rate can be calculated for non-reactive trials by setting $\frac{dQ_c}{dt}$ to zero to produce Equation (3).

$$\frac{dQ_{ht}}{dt} = -\frac{V}{\gamma - 1}\frac{dp}{dt} \quad (3)$$

Experiments without injection demonstrate that the heat loss rate during the period of interest after compression can be approximated as a constant value, which is calculated to be 191 J/s. This quantity is small relative to the peak heat release rates calculated for the reactive trials.

2.3 Accelerated Failure Experiments

Previous studies that have investigated hot surface ignition in CI engines have often cited over-voltaging these devices to achieve adequate performance [32-34]. The applied voltage is increased well beyond the nominal value to raise surface temperatures for extended periods of time, and significant reductions in lifetime and durability have been reported as a result. Durability experiments are challenging to conduct because testing in a research engine requires significant investment of time and resources and the in-engine environment is difficult to simulate. In order to study durability in a feasible manner, several experiments are designed and carried out in this study to provide insight into heating element failure modes.

The preliminary durability experiments are performed on the benchtop at atmospheric conditions. Voltages above the nominal value are selected to accelerate the degradation process to reasonable testing times. Using a closed loop current sensor, the current through the device is logged with a LabView data acquisition system. This data is used to determine the time to failure of the device, when current through the device deviates significantly from normal operation. Four voltages are tested, starting at 13 V and decreasing to 10 V in 1 V increments.

To better replicate the in-cylinder environment of light-duty CI engines, a 5,500 W portable diesel generator was modified to accommodate the hot surface device for extended runtime experiments. The goal of this experiment was to evaluate the degradation trends at nominal voltage in a realistic engine environment over a long runtime. It was determined that the

heating element could be introduced into the cylinder through the cylinder head with a custom mounting sleeve. The device was secured below the injector, angled at 55° to the normal as shown in Figure 10. This geometry results in the heating element tip protruding 5 mm into the combustion chamber, 15 mm from the injector nozzle tip.

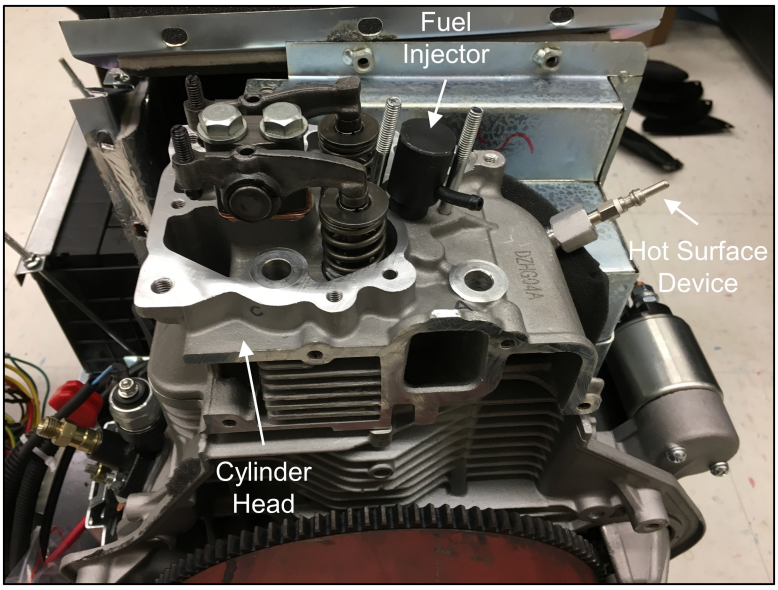

Figure 10. Single-cylinder diesel generator head modified to accommodate hot surface device

The heating element is powered from the 120 VAC outlet on the generator. An AC to DC converter is used to produce a constant 20 V and a variable voltage buck converter steps the voltage down to the desired nominal value. To ensure high-load operation, two 1500 W outdoor heaters were also powered by the generator AC output and set to run at maximum output throughout the entire experiment. The generator is fueled with standard automotive #2 diesel.

The third study to assess device durability is an accelerated failure experiment conducted in the RCM. This study is designed to investigate durability in a controlled manner while including combustion and thermal cycling that would be encountered in an actual engine. The heating element is secured in the RCM combustion chamber with the maximum allowable insertion depth, with the heating element tip 2.5 mm past the nozzle centerline. The in-cylinder

air is compressed to 40 bar, 900 K and F-24 fuel is injected with significant impingement of the fuel jet on the heating element surface. The heating element is activated at elevated voltage, and the RCM is operated until heating element failure occurs. Two trials were conducted, at 11.5 V and 11 V. The time and number of cycles until failure are recorded, and the resulting failure modes are analyzed.

CHAPTER 3: RESULTS AND DISCUSSION

3.1 Heating Element Performance

The benchtop startup performance of eight different brands of metal heating elements is shown in Figure 11. The thermocouple was placed 1 mm from the tip to ensure comparability between the different models. The results demonstrate relative similarity in the startup times and peak surface temperatures across the range of heating element brands.

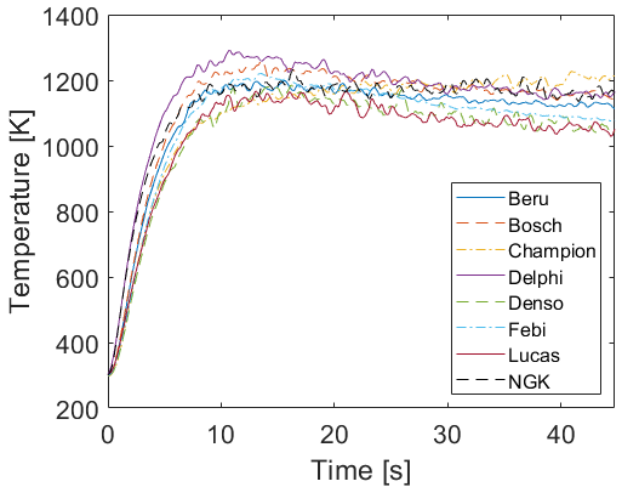

Figure 11. Startup performance of various COTS metal heating elements at ambient conditions

The performance of these heating elements is clearly optimized for the first 30 seconds of operation; they are not designed to be used for extended time periods after the engine has started. This is evident from Figure 11 which shows the peak temperatures are achieved 10-15 seconds after startup before decreasing to a steady state value. For older passenger car CI engine operation, heating during the first 30 seconds is most beneficial to performance, although these devices can be activated for up to 3 minutes if necessary.

On the other hand, some modern ceramic heating elements have been designed to support operation well after the engine has started. In order to reduce emissions and support regeneration of diesel particle filters, ceramic heating elements are operated continuously for up to 15 minutes

[8]. The superior performance suggests that they will be more relevant for spray ignition experiments. Figure 12a shows the temperature rise during startup of a Bosch ceramic heating element and the associated time constant, determined using nonlinear least squares regression.

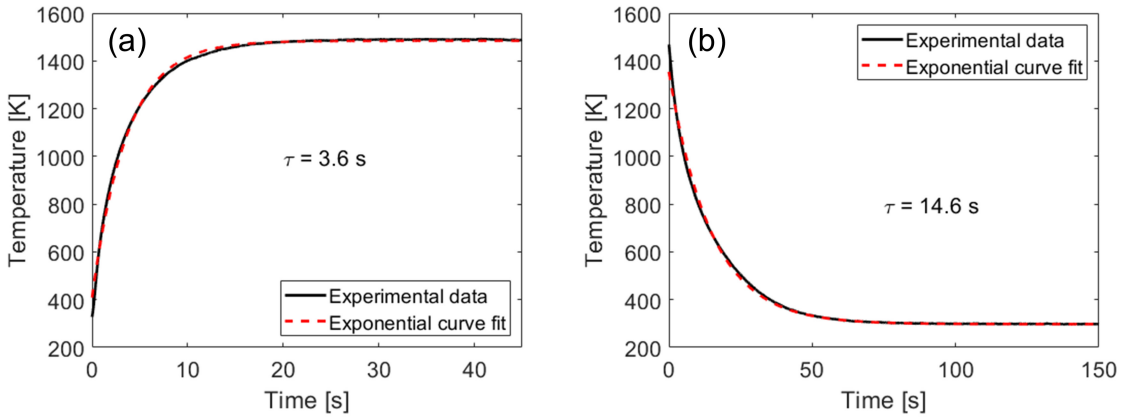

Figure 12. Startup performance and of Bosch 0250603008 ceramic heating element at ambient conditions (a) and cooldown behavior (b) with exponential time constants determined using nonlinear least squares regression

As expected, the ceramic heating element reaches higher temperatures in a shorter time period than the older-technology metal heating elements. The higher peak temperatures and monotonic temperature behavior during startup make ceramic heating elements ideal for spray ignition testing, where a wide range of desired temperatures can be directly correlated to the time after which voltage is first applied. Figure 12b shows the cooldown process from steady state after the applied voltage is turned off. This decay in temperature exhibits significantly longer time constants as the heating element is cooled primarily through natural convection.

Selecting this ceramic heating element for the remaining experiments, it is important to further characterize its performance. Figure 13a shows the startup performance at ambient temperature and pressure with different applied voltages. The device is tested in increments of one volt up to the nominal voltage of seven volts. This again demonstrates relatively long startup times and indicates that these devices are not suitable for fast-response ignition control schemes.

With existing heating elements, other parameters, including injection timing, will need to be utilized as actuators in order to achieve cycle-to-cycle control.

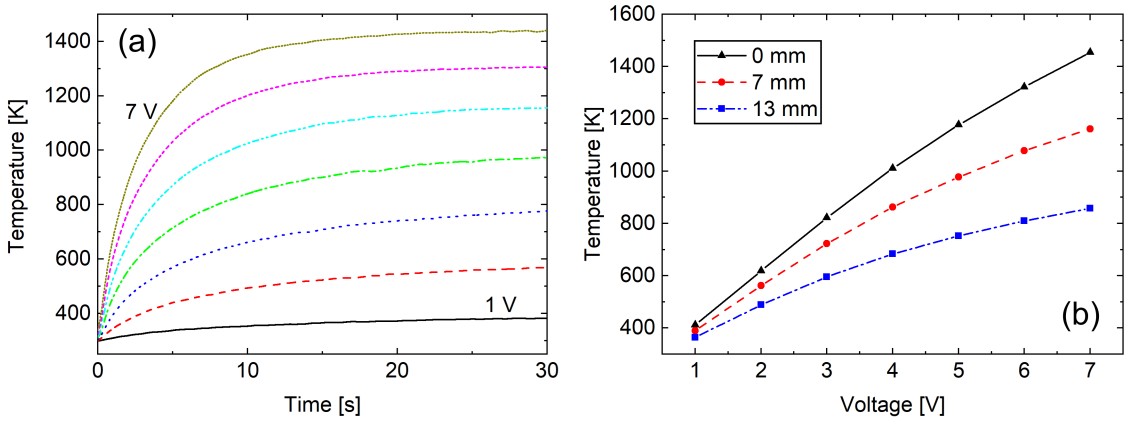

Figure 13. Heating element tip surface temperature at startup with different applied potentials (a) and steady state surface temperature at different distances from heating element tip (b) both at ambient conditions

The steady-state surface temperature of the device at three different distances from the heating element tip is shown in Figure 13b. Heating during startup occurs near the device tip, and heat is transferred through conduction to the rest of the heating element body. These results demonstrate that at steady state operation, a temperature gradient persists through the heating element surface. Positioning the device to maximize heat transfer to the ignitable mixture in-engine is an important consideration for optimizing ignition performance.

Figure 13b also demonstrates that the maximum surface temperature with the nominal voltage applied is about 1500 K. Accounting for cooling of the heating element due to the intake charge and cold liquid spray impingement, the temperatures of the heating element inside the engine are expected to be greatly reduced. Experiments in the literature cite over-voltaging these devices to achieve adequate performance. However, the higher internal temperatures significantly reduce device lifetime. Considering the increased power requirements and durability issues, existing heating elements are clearly not designed for continuous ignition-assisting operation at elevated surface temperatures.

3.2 Fuel Spray Ignition Measurements

F-24 Fuel Ignition Delay

The primary fuel of interest to the Army is F-24, a Jet-A fuel with military additives. This fuel has been adopted as the standard for gas turbine engine operation, and represents the first step towards enabling operation of CI engines with kerosene based fuels. It is fairly reactive, exhibiting a cetane number around 48.5 [28]. In order to establish baseline performance of the heating element in supporting spray ignition, F-24 is selected as the fuel for the first set of experiments.

The pressure recovery ignition delay of the fuel spray with varying heating element surface temperature is shown in Figure 14a. Three trials are performed for each condition and the average value is plotted. Conditions with high variability in the three trials are repeated three more times. These conditions are denoted with range bars indicating the maximum and minimum ignition delay measured along with the average value of the six trials. The maximum standard deviation for the trials with low variability is 0.06 ms.

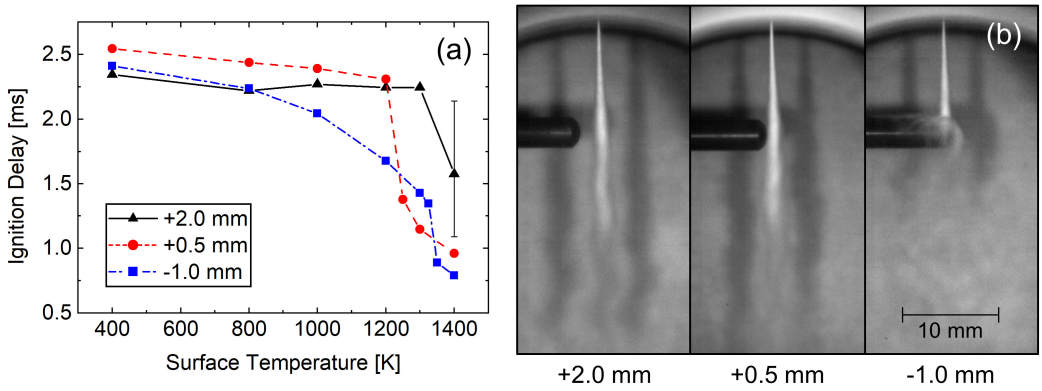

Figure 14. Ignition delay with heating element inserted at three different distances from the spray axis (a) and dual-halogen lamp front-illuminated 30 kHz images of fuel spray impingement (b)

Figure 14a demonstrates a sharp drop in ignition delay time at higher heating element surface temperatures. For the -1.0 mm and +0.5 mm distances from the spray axis, the heating

element is sufficiently close to transfer heat to the fuel vapor region surrounding the liquid core. At these positions, surface temperatures above 1250 K reduce the ignition delay to times that are practical for use in actual engines. With the heating element inserted 1 mm past the spray axis however, the spray structure is disrupted by impingement on the surface as seen in Figure 14b. In an engine, repeated injection events on the hot surface would result in extreme cooling and increased erosion. With the tip located 2 mm from the spray axis, the heating element is too far from the periphery to consistently improve ignition even at 1400 K. The highly sensitive performance differences over small changes in insertion depth emphasize that the influence of the hot surface is not global heating of the in-cylinder gases, but rather local energy deposition in the thermal boundary layer. These results conclude that the optimal configuration for a balance of performance and durability is the +0.5 mm position, which will be utilized for the rest of this study.

Ignition Mode Comparison

Imaging is performed to identify potential causes for the disparate ignition behavior over small changes in surface temperature above 1200 K. Figure 15 shows the ignition event of the +0.5 mm insertion depth at two different surface temperatures, with times indicated ASOI. This figure demonstrates a large variation in ignition location and broadband chemiluminescence intensity.

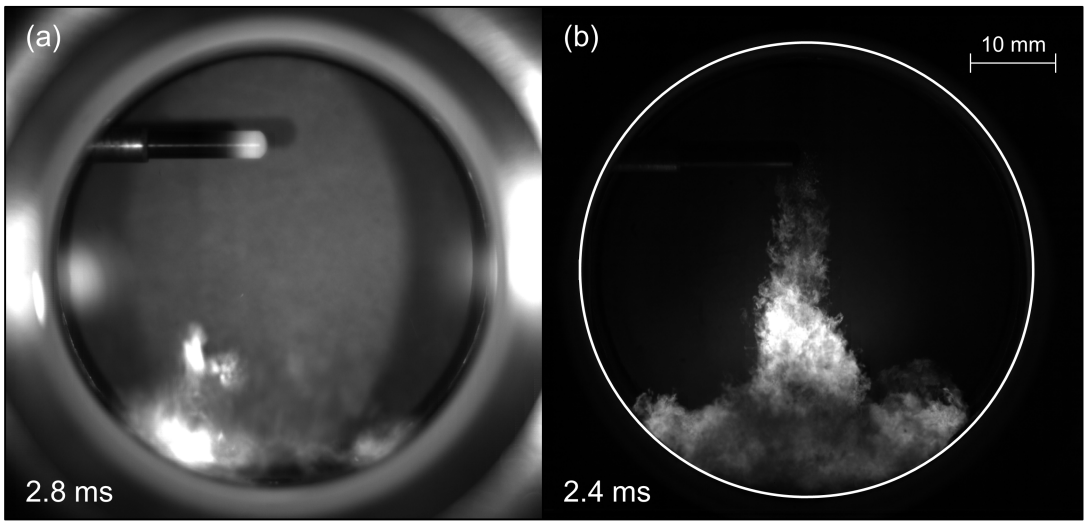

Figure 15. Broadband chemiluminescence images of two ignition modes with in-cylinder conditions 30 bar, 800 K: volumetric ignition at 1200 K surface temperature (a) and spray ignition at 1250 K surface temperature (b), times indicated ASOI

Because of the distinct behavior of these two cases, they will be referred to as different ignition "modes." At lower surface temperatures, the mixture ignites after the injector has closed in a near-premixed fashion. Ignition occurs at the bottom of the chamber, as seen in Figure 15a. The combustion event proceeds rapidly and propagates throughout a large mixture volume. It is characterized by a relatively low broadband luminescence intensity and will be called "volumetric ignition." The second ignition mode is common to diesel fuel sprays at high-pressure and temperature compressed conditions and will be referred to as "spray ignition." This mode, shown in Figure 15b, occurs in a fuel rich region and displays high signal intensity. Figure 16 demonstrates the significantly different heat release behavior of the two ignition modes. A digital Butterworth filter with a cutoff frequency of 3,000 Hz is used to condition the derivative of the raw pressure signal.

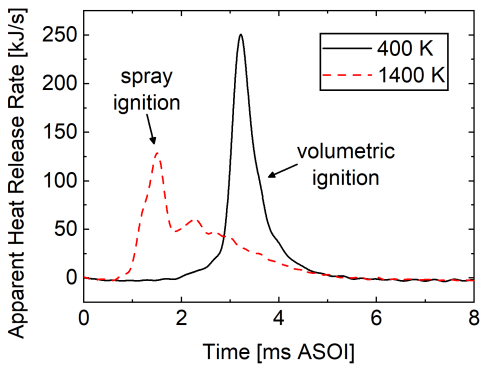

Figure 16. Comparison of heat release rate of volumetric ignition (solid) and spray ignition (dotted) observed at different heating element surface temperatures

The heat release rate profiles demonstrate that at increased surface temperature, the combustion event initiates faster and is distributed over a longer burn duration. The volumetric ignition heat release profile is indicative of that encountered with HCCI combustion, where the fuel and oxidizer are partially mixed before a violent release of heat energy occurs as the mixture ignites. The large pressure rise rate and associated knocking is undesirable for HCCI engines operated at high loads [35]. Transitioning from premixed combustion with low emissions to spray combustion with efficient fuel use through the control of heating element surface temperature is an interesting concept for the low temperature and pressure conditions evaluated in this study.

Spray Ignition Analysis

For the +0.5 mm case, where the heating element tip is located in the spray periphery, broadband chemiluminescence imaging is performed to examine the effects of surface temperature on flame kernel formation for the “spray ignition” mode. Figure 17 depicts formation of a local ignition flame kernel near the heating element tip that propagates to the lift-off length (LOL). The signal is greater on the left side of the spray, directly downstream of the heating element. The final frame demonstrates that flame propagation occurs through the center

of the spray only after the flame reaches the LOL. At this location, most of the liquid core is vaporized and there is a large volume of ignitable mixture that is accessible to the flame front.

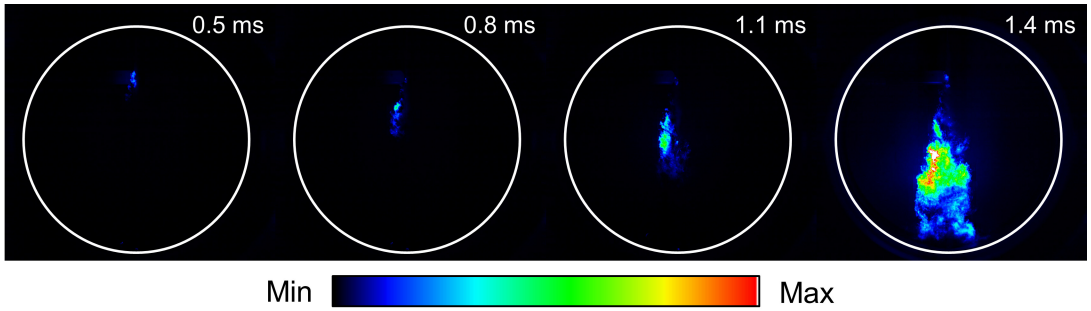

Figure 17. Broadband chemiluminescence image sequence with heating element inserted 0.5 mm from spray axis, 1400 K surface temperature, times indicated ASOI

The flame kernel location and size as a function of time after the start of injection are shown in Figure 18 and Figure 19, respectively. Three trials for each condition are shown to demonstrate the repeatability of the measurements. The image set was binarized using a 16-bit threshold of 5,000 counts, and the single largest contiguous area for each frame was selected and defined to be the flame kernel. The frame before the flame area exceeded 75,000 pixels (375 mm2) was selected as the limit for the plots, which correlates well to luminosity in the majority of the spray structure and the transition from a “kernel” to a fully ignited spray.

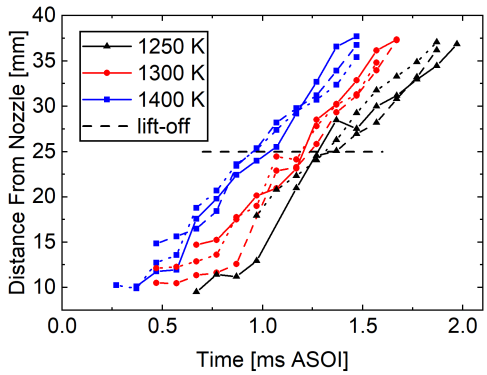

Figure 18. Propagation of local-ignition flame kernel for three different trials at three surface temperatures

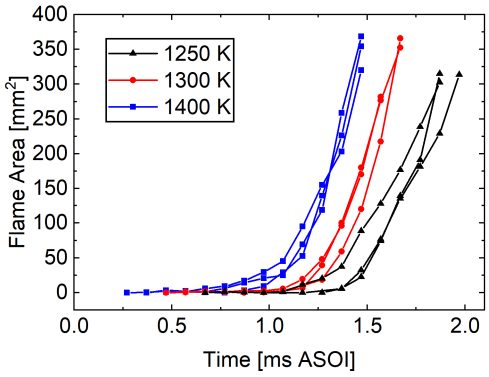

Figure 19. Growth of local-ignition flame kernel for three different trials at three surface temperatures

For the +0.5 mm case, Figure 14 indicates that the ignition delay decreases for surface temperatures increasing from 1250 to 1400 K. Figure 18 and Figure 19 demonstrate the mechanism by which ignition delay is accelerated. At higher heating element surface temperatures, the flame kernel originates farther upstream and earlier in time than the lower temperature cases. The increased surface temperature accelerates chemical reactions of the fuel vapor/air mixture in the device thermal boundary layer. Once an ignition kernel is formed, the flame propagates downstream along the ignitable mixture region surrounding the liquid core. When it reaches the LOL, the liquid core has mostly evaporated and a large volume through the center of the spray can ignite, as indicated by the significant increase in flame kernel area. Combustion around the LOL corresponds to global pressure rise within the chamber, despite the formation of flame kernels up to a millisecond prior.

For the conditions studied here, Figure 18 demonstrates that the flame kernel is advected downstream with an average velocity of 23 m/s and is not a strong function of surface temperature. This value is two orders of magnitude greater than the laminar flame speed of kerosene reported in the literature, and is influenced by the local flow velocity, turbulence, and spray physics [36].

Pressure recovery ignition delays in Figure 14 correlate well with the time at which the flame kernel reaches approximately halfway down the cylinder, at 25 mm from the nozzle tip as shown in Figure 18. For the short duration of injection utilized (1.5 ms), this location corresponds to the approximate flame LOL observed from imaging. When the flame kernel reaches the LOL, significant growth in flame kernel area and signal intensity is observed. This phenomenon is different than that observed with a laser spark induced upstream of the natural LOL, where ignition occurs at the spark and the LOL decays exponentially to the steady state value [37]. However, no pressure data was provided to correlate chemiluminescence signal with heat release in [37]. The rate of energy deposition of a hot surface is much slower than that in a laser spark, and short residence times of the mixture in the vicinity of the heating element surface limit the total amount of energy that can be deposited [26]. A comparison of the heat release profiles for a single trial at each surface temperature is provided in Figure 20.

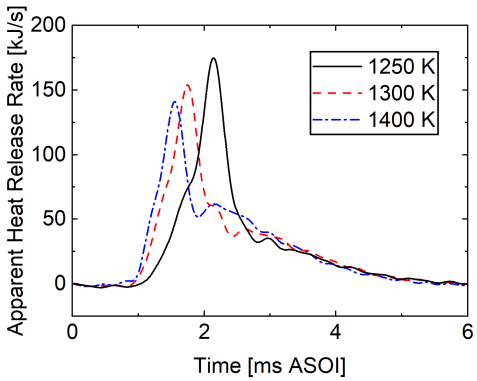

Figure 20. Heat release rate profiles of F-24 fuel spray at three heating element surface temperatures

The general trends of heat release correlate well with flame area and ignition delay. The time at which peak heat release occurs is accelerated at higher heating element surface temperatures. In addition, the value of peak heat release rate decreases as surface temperature is increased. This trend extends to lower surface temperatures and the volumetric ignition mode,

where significantly larger peak heat release rates are observed. Figure 20 suggests that the timing of peak heat release in an engine can be modified by controlling surface temperature.

Cetane Fuel Ignition Delays

With baseline performance established, cetane fuels with different reactivity but similar physical properties can be used to study the feasibility of utilizing a hot surface device to accelerate ignition of low-quality fuels. The pressure recovery ignition delay measurements at heating element surface temperatures ranging from 400 K to 1400 K are shown in Figure 21. When the heating element tip temperature is at 400 K (not powered) or at the ambient in-cylinder air temperature of 800K, the ignition delay is nearly identical to the performance without the heating element inserted. At these low surface temperatures, where the effect of the heating element is negligible, a clear difference in reactivity is evident in the CN 30 fuel. Interestingly, the ignition delay of CN 35 and CN 40 are comparable at these conditions, despite differences in cetane number. This can be attributed to similar first-stage ignition heat release that is evident from the heat release rate profiles. Multi-stage ignition of these fuels has been analyzed for homogeneous mixtures in Ref. [27].

For the experiments conducted in this study, the pressure-recovery method results in the first-stage ignition delay being reported as the overall ignition delay, even though second-stage ignition with larger heat release may be of greater interest for optimizing injection timing in-engine. However, the long ignition delays associated with low surface temperatures are impractical for single-injection operation. Studying ignition performance at these conditions is more useful for understanding the behavior of pilot injection and combustion, where two-stage ignition may be observed for low-reactivity fuels.

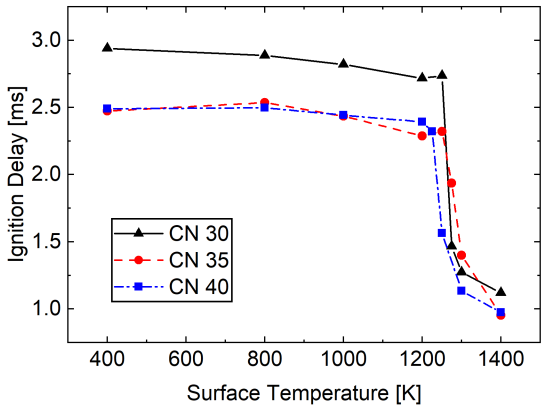

Figure 21. Pressure recovery ignition delay of varied cetane number fuels at 30 bar, 800 K over a range of heating element surface temperatures

At surface temperatures of 1000 K and 1200 K, a small decrease in ignition delay is observed. This likely occurs due to slightly increased evaporation and accelerated chemical kinetics as the hot surface transfers heat to the spray and surrounding vapor cone. Because of the fast spray velocity, residence times in the device thermal boundary layer are small and the effect of the hot surface is limited.

Above surface temperatures of 1200 K, a sharp decrease in ignition delay time is apparent. The decrease in ignition delay is also observed for the F-24 fuel experiments at the same surface temperatures. This behavior corresponds to enough heat transfer within the short mixture residence time to ignite the spray while injection is still occurring. Ignition delays below 1.5 ms exhibit typical diesel engine spray combustion behavior, which involves a premixed burn phase followed by a mixing-controlled combustion phase [38].

At heating element surface temperatures of 1300 K and 1400 K, the ignition delays approach 1 ms. The convergence of the ignition delay to a similar value implies reduced sensitivity of ignition performance on cetane number. This phenomenon corresponds to the transition from low temperature chemistry experienced at the 800 K ambient compressed

temperature to high temperature chemistry-dominated behavior when the hot surface supplies sufficient energy to the mixture.

Broadband Chemiluminescence Imaging of Cetane Fuels

In order to study the interaction between the heating element and fuel spray, broadband chemiluminescence imaging is performed while the chamber is illuminated with a halogen lamp. To correlate imaging and pressure data, all times are indicated ASOI. Figure 22 depicts a series of images from a single injection event of CN 35 with a heating element temperature of 1200 K.

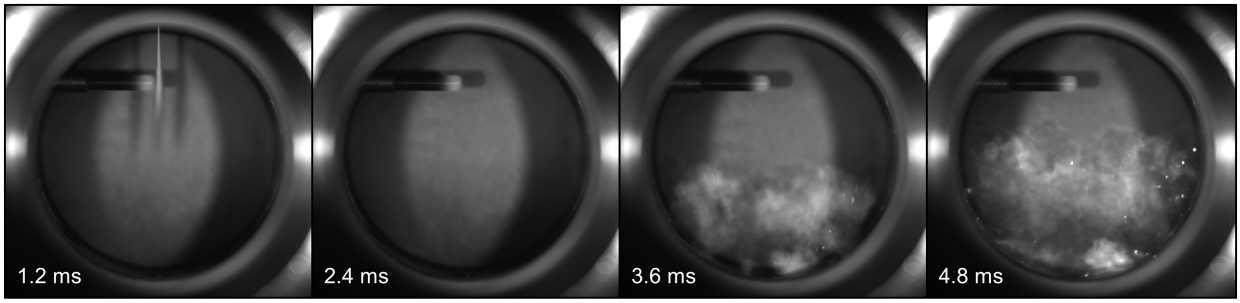

Figure 22. Broadband chemiluminescence image sequence of CN 35 fuel, heating element surface temperature 1200 K, illuminated with halogen lamp, times indicated ASOI

At 1.2 ms ASOI, injection has reached quasi-steady behavior, and the spray is visible due to elastically scattered light from the halogen lamp. The injector closes and the fuel is completely evaporated before 2.4 ms ASOI. At this point, the ignition behavior approaches that of a homogenous mixture, and by 3.6 ms significant chemiluminescence signal is visible as the mixture ignites from the bottom of the chamber. Combustion proceeds through the majority of the cylinder by 4.8 ms ASOI. Figure 22 indicates that for lower heating element surface temperatures, the mixture ignites after the injector has closed in a near-premixed fashion.
At the low surface temperature conditions, ignition determined from the pressure trace occurs before the first detected chemiluminescence signal. The discrepancy in ignition delays is due to first-stage heat release, which does not result in high signal intensity. The first-stage heat release

is sufficient to overcome pressure loss due to vaporization but does not correlate to luminescence signal and the onset of peak heat release.

Cetane Fuel Heat Release Rate Analysis

In order to examine the discrepancy between ignition delays from pressure recovery and imaging, the apparent heat release rates are analyzed. Figure 23a shows the heat release behavior of the unassisted spray. The plot clearly demonstrates two heat release events, which represent first-stage and second-stage ignition. The heat release of the low-reactivity CN 30 fuel is distributed over a long duration, and the first stage is delayed relative to that of the higher-reactivity fuels. The first-stage heat release of CN 35 and CN 40 occurs at similar times, which accounts for similar pressure recovery ignition delay times. However, it is clear that the main heat release event occurs faster for the CN 40 fuel.

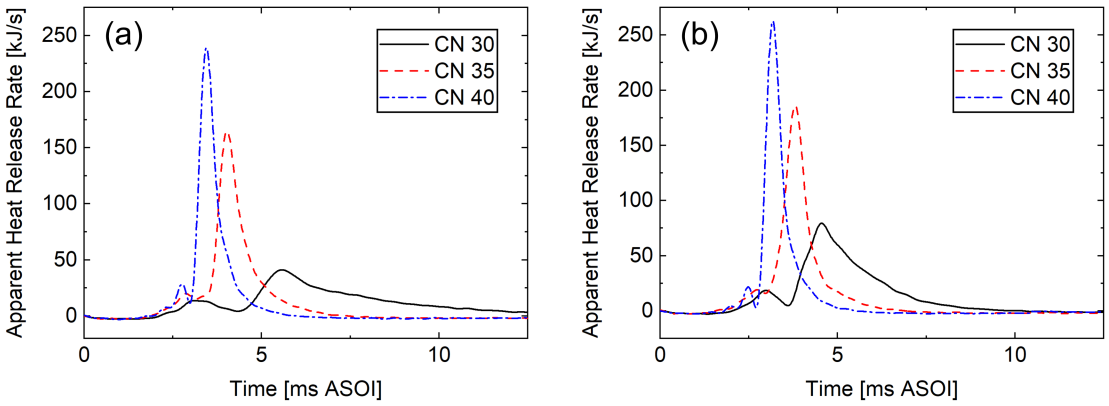

Figure 23. Differences in apparent heat release rate of varied cetane number fuels with heating element surface temperatures of 400 K (a) and 1200 K (b)

At a higher heating element surface temperature of 1200 K, the heat release of the three fuels follows the same trends as shown in Figure 23b. Energy supplied by the hot surface accelerates the first-stage ignition event and results in a shorter ignition delay. The hot surface also serves to increase the peak heat release rates of all three fuels.

Ignition delay times with a surface temperature of 1400 K converge towards 1 ms. Figure 24 compares the heat release behavior of the fuels with a surface temperature of 1400 K. At this temperature, the heat release behavior between the fuels is similar. The first-stage ignition event is no longer present, and the peak heat release rates are smaller than at lower surface temperatures.

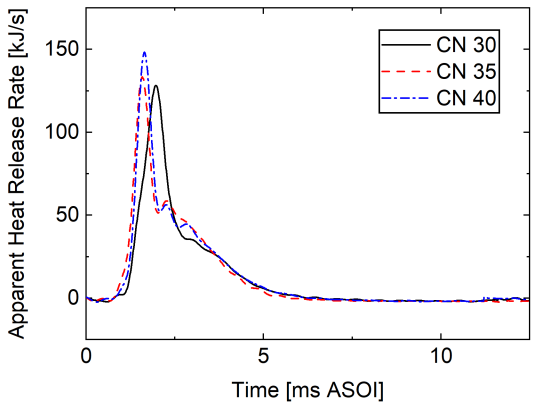

Figure 24. Apparent heat release rate of varied cetane number fuels with in-cylinder conditions of 30 bar, 800 K at heating element surface temperature of 1400 K

This combustion behavior corresponds to that of a traditional diesel spray. An initial peak in heat release rate is evident due to the premixed combustion phase. Injection ends before the spray combustion process transitions to the typical “mixing-controlled” combustion phase that results in a moderate increase in heat release rate. Figure 25 depicts a rate of heat release diagram for a diesel engine that demonstrates the different phases of combustion.

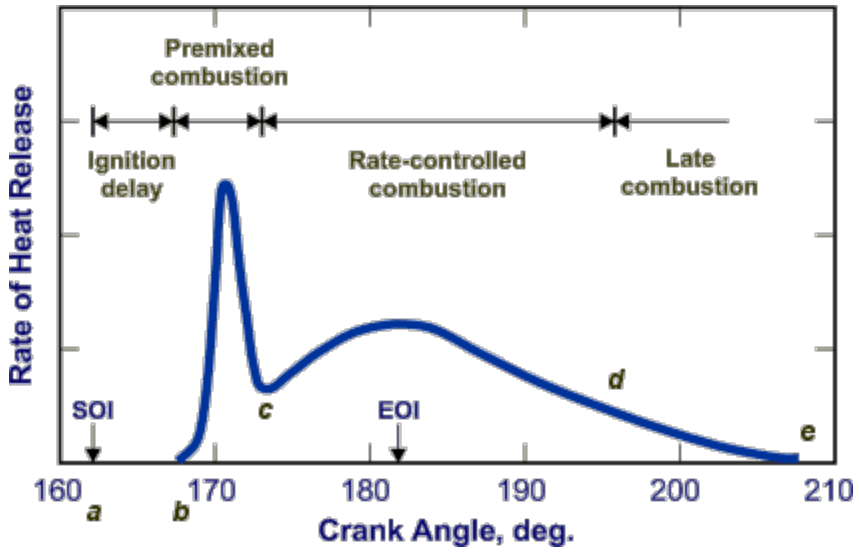

Figure 25. Rate of heat release diagram of diesel fuel spray [38]

At the 1400 K surface temperature, the effect of cetane number is greatly reduced and the heat release profiles are comparable. The hot surface provides sufficient energy to support high temperature chemical pathways that result in similar ignition behavior.

3.3 Durability Assessment

Benchtop Experiments

Analyzing potential failure modes of existing heating elements is important for designing novel ignition systems. The simplest and most accessible study to conduct is benchtop testing of lifetime at ambient conditions with elevated surface temperatures. The time to failure of the ceramic heating element at four different voltages is shown in Table 3.

Table 3. Durability of Ceramic Heating Element at Ambient Conditions

Voltage [V]	Time to Failure
13	38.6 seconds
12	4.4 minutes
11	24.6 hours
10	> 2 weeks

The lifetimes of the heating elements vary significantly over the range of tested voltages. For the 10 V trial, the device had not yet failed when the test concluded at the end of two weeks.

Figure 26a shows the heating element before it has been tested without voltage applied. It is used to compare with images of the heating elements after failure to identify damage caused by the durability experiments. Figure 26b depicts the heating element before durability testing at steady state with the nominal voltage applied.

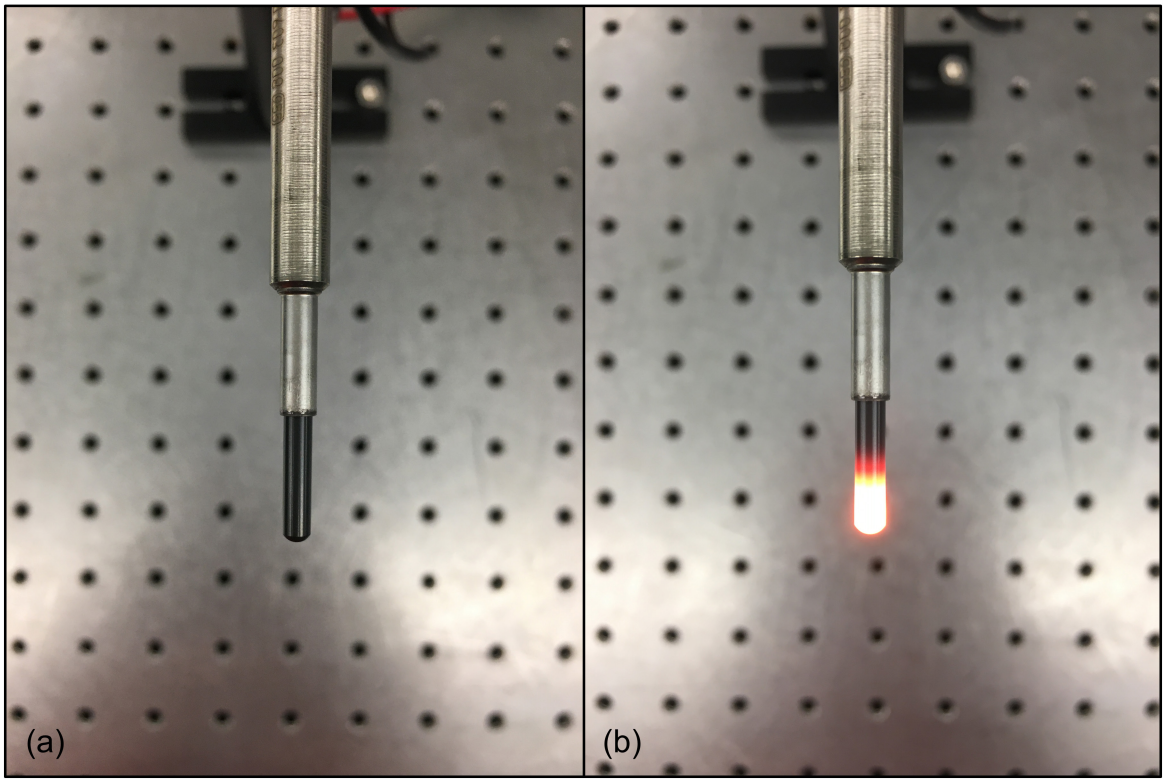

Figure 26. Unpowered Bosch 0250603008 ceramic heating element (a) and heating element at steady state with nominal voltage applied (b)

With an applied potential of 13 volts, the heating element fails before the surface temperature reaches a steady state value. Figure 27 shows the surface temperature at the base of the heating element and the current through the device for the 13 V case during startup. The failure mode associated with this case is an “overheating” mode, which involves two distinct processes.

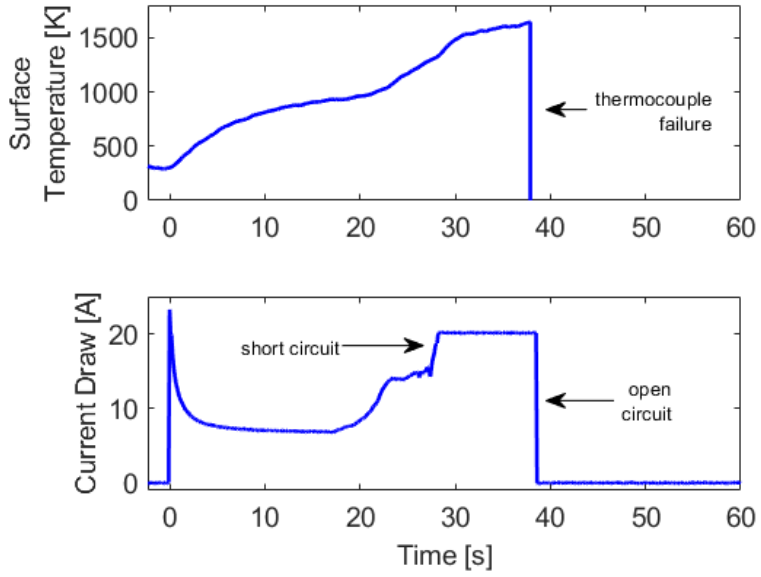

Figure 27. Overheating failure mode during 13 V benchtop experiment utilizing 20 amp regulated power supply, time indicated after voltage is first applied

Due to the increased current through the device as a result of the large applied potential, the high internal temperatures cause the conducting element to fail. A short circuit is formed, whereby the device pulls as much current as possible from the supply and the device is heated even further. The extreme temperatures experienced at this stage cause the ceramic structure to expand and the internal conductor to fail entirely, resulting in an open circuit. At this point, the heating element has been destroyed and resistive heating can no longer occur.

The results of this failure mode can be seen in Figure 28. The tip of the heating element has expanded outwards as shown in Figure 28a and some of the ceramic material has experienced embrittlement. Figure 28b demonstrates that the metal support tube at the base of the heating element has melted, indicating that extreme temperatures are experienced both at the heating element tip as well as the body of the device.

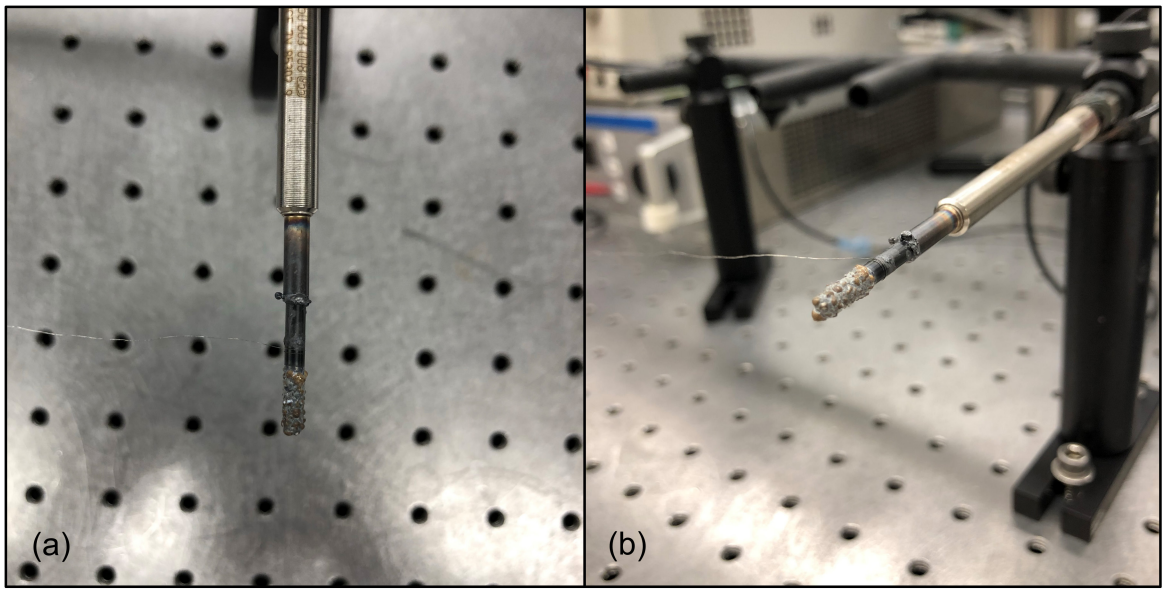

Figure 28. Failed ceramic heating element after 13 V benchtop durability experiment, elongated heating element tip (a) and deformed support tube (b)

For the 12 V test, failure also occurs in an overheating mode, although it takes longer for the device to short circuit. The internal temperature encountered at this voltage can be sustained for a longer period of time until the internal heater has been compromised. Figure 29a shows the failed heating element for the 12 V case, where significant expansion of the heating element is observed. A greater portion of the ceramic surface is damaged, whereas less of the metal support tube has melted.

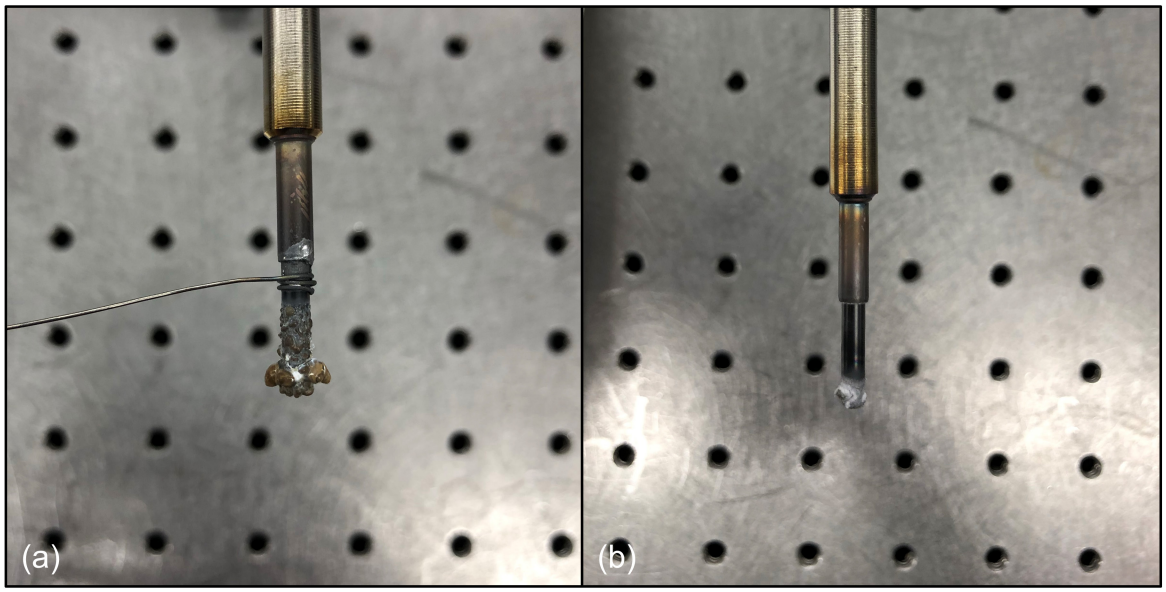

Figure 29. Failed ceramic heating element after 12 V benchtop failure experiment (a) and 11 V experiment (b)

Figure 29b shows the failed heating element of the 11 V trial. The failure time for this case exceeds 24 hours, which is significantly longer than the previous two trials. Damage to the ceramic material is observed at the heating element tip, although most of the heating element remains intact. Oxidation of the silicon nitride ceramic at the tip is also visible. The metal supporting structure shows no deformation due to the elevated heat element temperatures. With 11 V applied, the steady state current is 5.9 A. The current decreases slowly throughout the testing period to 4.4 A, after which an instantaneous drop to less than 1 A occurs and the device no longer produces significant heat, denoting failure.

The final test case for the benchtop experiments is the 10 V trial. No failure was observed before two weeks, after which the experiment was concluded. Figure 30 shows the 10 V trial heating element after two weeks, for which the current through the device remained at the steady state value of 5.7 A.

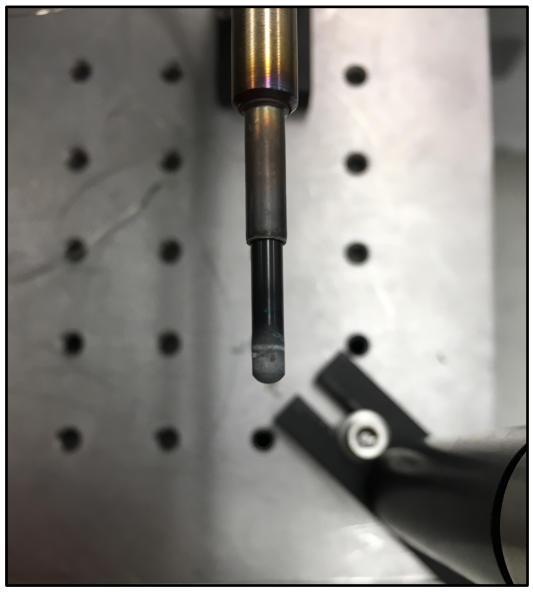

Figure 30. Oxidation of operational ceramic heating element after 2 weeks for 10 V benchtop durability experiment

Significant oxidation of the first 5 mm from the heating element tip is visible, and no significant damage to the heating element is apparent. It is estimated that the internal temperatures experienced at this condition are insufficient to melt the internal conducting structure so the heating element will not experience an overheating mode. Failure at this voltage is more likely to occur due to long-term degradation.

Diesel Generator Degradation Test

Benchtop testing provides a good baseline for assessing heating element durability, but it is not representative of an actual engine environment. Thermal cycling due to rapid changes of the in-cylinder conditions, impingement of the cold fuel spray, and the rapid temperature rise associated with combustion all require that ceramic materials selected for heating elements have adequate thermal shock resistance. Modifications made to a diesel generator allow for examining heating element degradation in a realistic environment over relatively long periods of runtime. The study is conducted for a total runtime of one week with the nominal 7 V applied to the device. Images of the heating element after the study has concluded can be seen in Figure 31.

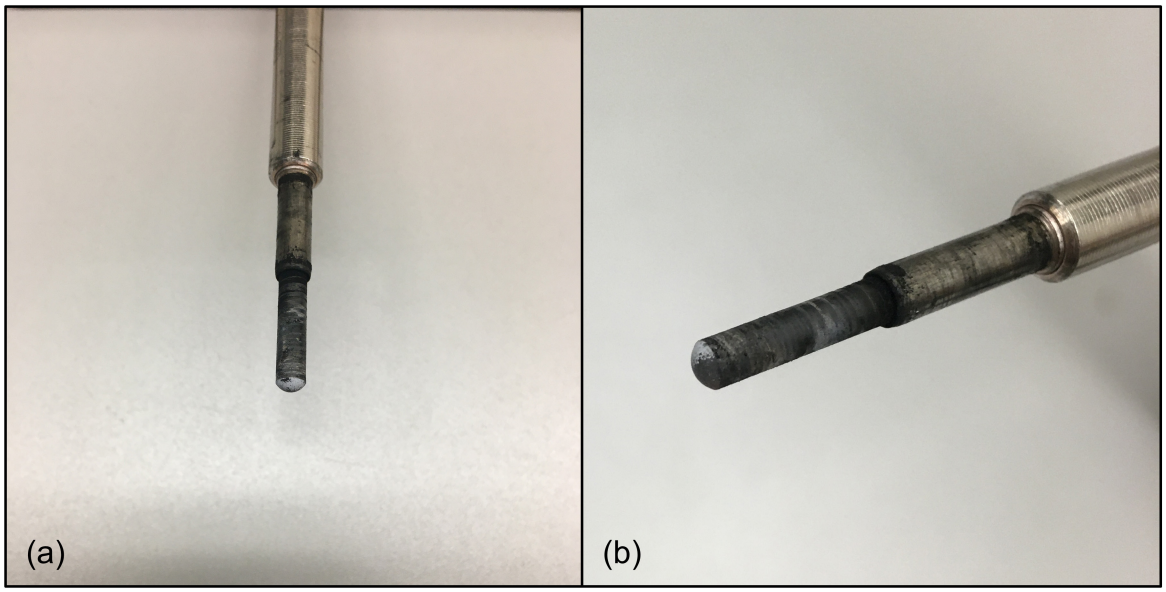

Figure 31. Operational heating element after 1 week of generator durability experiment with nominal 7 V applied (a) and closeup of preferential oxidation of heating element end face

There is minimal degradation to the heating element despite exposure to the harsh engine environment. Figure 31 demonstrates that soot buildup is limited and there is little to no soot present at the tip of the device. Slight oxidation of the ceramic is apparent, especially on the end face of the tip. The end face exhibits preferential oxidation to one half of the surface, indicating that the side exposed directly to the fuel spray will deteriorate faster over an extended testing time. The lower surface temperatures associated with the nominal applied voltage result in reduced degradation of the heating element surface and a failure mode that is more likely to occur after extended operation.

RCM Failure Mode Experiments

The well-controlled compression and injection event of the RCM can be utilized to simulate thermal cycling and combustion encountered during actual heating element operation. Although CI engines can cycle thousands of times per minute, the voltage of the heating device can be adjusted for RCM durability experiments so that different heating element failure modes can be studied. Two trials are performed, at voltages of 11.5 V and 11 V. Table 4 shows the

operation time and number of RCM compression and injection events carried out before failure. It also compares lifetimes with the benchtop experiments at the same voltage. An exponential curve fit is used to interpolate the expected benchtop lifetime at 11.5 V, using the data collected at 11 V, 12 V, and 13 V.

Table 4. Results of RCM Accelerated Failure Experiments

Voltage [V]	Number of Injections	Time Until Failure [min]	Percent Change from Ambient
11.5	2	4.5	-96 %
11	180	217	-85 %

The lifetime comparison reveals a large reduction in time to failure for both tested voltages. This suggests that the combined effects of spray impingement, thermal shock of the compression and combustion events, and vibration of the surrounding structure significantly reduce device durability compared to the ambient conditions. For the trial at 11.5 V, failure occurs too quickly to have been influenced by increased degradation of the heating element surface due to combustion. Only two injection events were performed in that time, so the reduced lifetime is due to a mechanical failure induced by the sharp pressure rise of the compression and combustion events as well as the associated vibration. Figure 32a shows the failed heating element in the inside of the combustion chamber after the 11.5 V test.

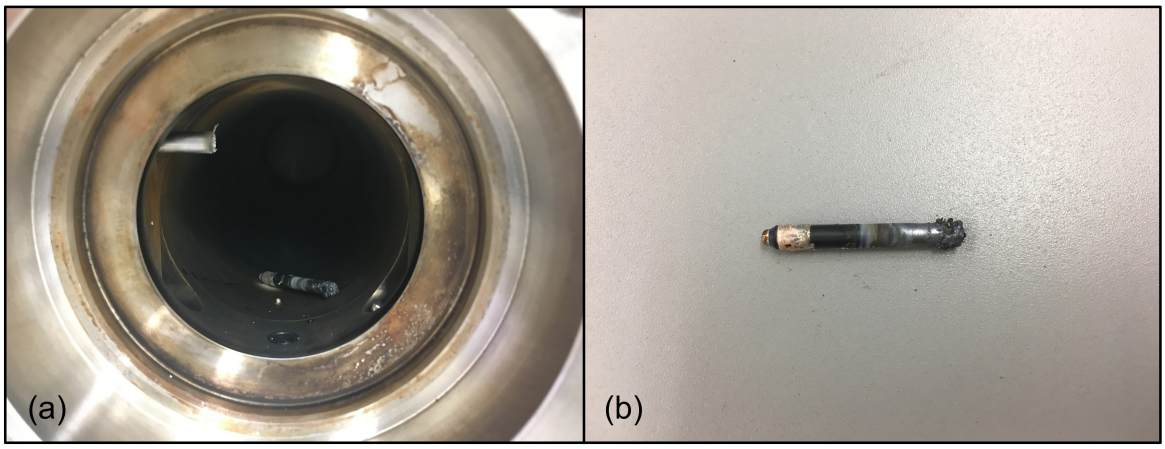

Figure 32. Heating element failure after 11.5 V durability experiment: inside of RCM combustion chamber (a) and detached heating element closeup (b)

This figure demonstrates that failure occurs at the connection terminal from the ceramic heating element to the device body. The increased temperatures due to over-voltaging weaken this connection, while operation of the RCM causes the heating element to break free from the supporting metal tube. Figure 32b shows that the heating element exhibits some preliminary damage at the tip similar to the benchtop experiments, however the ceramic heating element remains intact.

The failure mode observed for the 11 V trial is significantly different. For this case, hundreds of cycles of compression and injection were performed, leading to significant oxidation of the ceramic surface. Figure 33a shows the heating element after failure and demonstrates that the heating element remains connected to the body of the device.

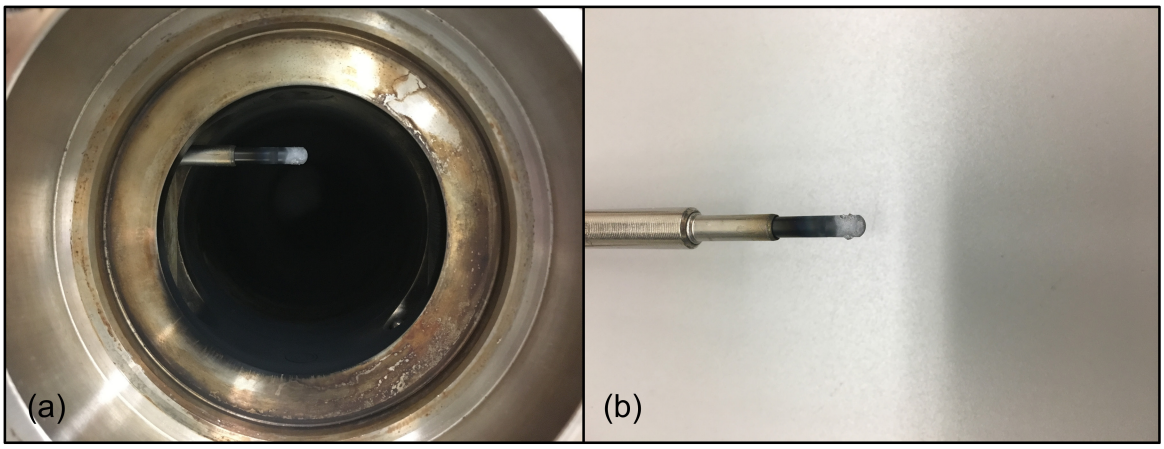

Figure 33. Heating element failure after 11 V durability experiment: inside of RCM combustion chamber (a) and heating element closeup depicting surface deposits (b)

Although erosion of the surface was expected due to impingement of the fuel spray, Figure 33b indicates a buildup of material on the heating element surface. This is likely due to the formation of silicate deposits on the surface and has been observed for relatively short testing times [39]. Failure for this trial occurs internally, indicated by an instantaneous 40 % drop in the current from the 6 A steady state value. This suggests breakdown of the conducting element and imminent failure of the device, although the device can still heat up with a reduced output power.

CHAPTER 4: CONCLUSION

4.1 Summary

The development of a multi-fuel capable CI engine is a challenging project that aims to provide improved operational flexibility to Army vehicles. A critical task for enabling reliable performance with low quality fuels is to design an ignition system that can reduce fuel spray ignition delay to feasible timescales; especially at the most extreme conditions where increased elevation and low-load operation result in slowed reaction rates and combustion instability. The present work provided an assessment of existing heating elements in functioning as hot surface ignition devices to support long term operation with kerosene fuels. Three distinct studies were conducted to evaluate several aspects of heating element performance.

The first study characterized the startup performance and maximum surface temperatures of heating elements when operating at ambient conditions, and found that heating time constants are insufficient to assist with cycle to cycle engine control. Designed temperatures do not exceed 1500 K, and convective cooling due to in-cylinder flows will reduce these temperatures in practical applications. Over-voltaging techniques have been applied to compensate for the effects of increased cooling at the expense of reduced durability.

Using the well-characterized startup performance of a Bosch ceramic heating element, the influence of surface temperature, geometry, and fuel reactivity on fuel spray ignition behavior was examined. When the heating element is placed in the periphery of the spray and surface temperatures exceeding 1250 K are achieved, the heating element can induce a local ignition flame kernel which will ignite the entire spray. This phenomenon results in a reduction of the ignition delay that can be sufficient to enable engine operation with a wide range of fuel reactivities.

Finally, in order to better understand the limitations of device durability, several experiments were carried out to assess failure modes in different environments. Observed failure can occur quickly due to overheating, or over an extended time period during which the internal conductor breaks down. Failure in realistic environments will most likely occur due to long term degradation of internal heater, although extreme erosion of the surface leading to conductor failure has been observed in some applications [33].

This work concludes that multi-fuel capable operation utilizing hot surface ignition devices is feasible with sufficient customization for a given engine. Ensuring adequate interaction between the heating element and spray while minimizing cooling effects is an important step in optimizing performance. Questions about device durability remain, including if a hot surface device can maintain requisite surface temperatures for the entire operational cycle while assisting ignition of very low reactivity fuels. Optimizing the design and ceramic materials for continuous use will be the biggest challenge in making hot surface ignition devices successful.

4.2 Recommendations for Future Work

The present work has emphasized the importance of material design in improving device performance. The material used currently as the ceramic sheath, silicon nitride, is well suited for the harsh engine environment and any improvements made to this material will likely be incremental in nature. It is for this reason that other solutions should be considered, including different ceramic materials or design structures. If erosion, oxidation, or corrosion proves to be a limiting factor to durability, environmental barrier coatings which maintain adequate heat transfer but protect the heating element from degradation should be considered. Some coatings have been used successfully in gas turbine engine applications which encounter similar high

temperature and pressure reacting flows [40]. Ceramic matrix composites can also be considered for a protective layer.

Another important design parameter is the heating element shield. Experiments in the present study considered spray interaction with a bare heating element, but many engine studies have utilized a shield to cover the surface and improve performance. Properly designed shields can reduce convective cooling, reduce impingement of the cold fuel spray, and increase residence time of the ignitable mixture in the device thermal boundary layer [26, 41]. Future experiments should investigate how to optimize shield geometry while maintaining adequate fuel/air mixing. An additional consideration is that because shields are typically a thin metal part surrounding the heating element, they can be coated with a catalytic material to accelerate the ignition process.

One large difference between the RCM and an actual engine is the shape of the compressed volume. Typical piston bowl geometry is quite different than the flat crown of the creviced piston used in the present study. In CI engines, the confinement of the fuel spray plume and the residence time of the fuel next to the heating element is likely much larger due to the effects of lip entrainment. Optimizing the equivalence ratio at the heating element surface for a variety of operating conditions will be critical to minimizing ignition delay times. Further studies in the RCM can evaluate the effect of vertical position, in addition to insertion depth, in influencing the equivalence ratio distribution. Another parameter to consider is the interaction of pilot-injected mixtures with the hot surface. Most modern engines utilize split injection strategies to improve ignition behavior and reduce emissions, however the present work considered only a single main injection. It will be important for future studies to quantify the effects of heating elements on pilot ignition with the increased confinement that a piston bowl provides.

Finally, the effects of turbulence and in-cylinder flows may influence ignition behavior in an engine. The RCM is a relatively quiescent environment, and the heating element is able to develop a thermal boundary layer before injection occurs. In an engine environment, convection and turbulence may reduce the boundary layer thickness. The size of this boundary likely plays an important role in the creation of local-ignition flame kernels, and may have an important influence on spray/heating element interaction. Furthermore, the turbulence intensity inside the combustion chamber, both influenced by the compression stroke and induced by the spray jet, plays an important role in kernel formation and flame propagation. Quantifying this value and studying its influence on overall ignition behavior is a unique avenue for further investigation.

REFERENCES

[1] M. Zheng, G. T, Reader, and J. G. Hawley, "Diesel engine exhaust gas recirculation—a review on advanced and novel concepts," *Eng. Conv. Mgmt.* 45, 883-900, 2004.

[2] H. Liu, S. Li, Z. Zheng, J. Xu, and M. Yao, "Effects of n-butanol, 2-butanol, and methyl octynoate addition to diesel fuel on combustion and emissions over a wide range of exhaust gas recirculation (EGR) rates," *Applied Energy* 112, 246-256, 2013.

[3] E. Hellström, A. G. Stefanopoulou, and L. Jiang, "Cyclic Variability and Dynamical Instabilities in Autoignition Engines with High Residuals," *IEEE Transactions on Control Systems Technology* 21 (5), 1527-1536, 2013.

[4] N. Yilmaz and B. Morton, "Effects of preheating vegetable oils on performance and emission characteristics of two diesel engines," *Biomass and Bioenergy* 35, 2028-2033, 2011.

[5] M. Pugazhvadivu and K. Jeyachandran, "Investigations on the performance and exhaust emissions of a diesel engine using preheated waste frying oil as fuel," *Renewable Energy* 30, 2189-2202, 2005.

[6] Motor Fan Illustrated Vol. 15, San'ei Shobo Publishing Co., Ltd., Jan 2015.

[7] G. V. Nolte and J. E. Smith, U. S. Patent for an "Ignition Plug," Patent Number 1,293,520, filed Jul. 26, 1918.

[8] Product Information Automotive Glow Plugs, Bosch Ltd., 2013.

[9] C. Havenith, H. Kuepper, and U. Hilger, "Performance and Emission Characteristics of the Deutz Glow Plug Assisted Heavy-Duty Methanol Engine," SAE Truck and Bus Meeting and Exposition, November, 1987.

[10] W. A. Goetz, and C. G. Barringer, "Utilizing Neat Methanol and Glow Plug Ignition in DI Diesels: Laboratory Testing of a Single and Multi-Cylinder Engine," *SAE Transactions* 103 (4), 711-726, 1994.

[11] U. Hilger, G. Jain, E. Scheid, F. Pischinger, R. Bruetsch, W. Bernhardt, H. Heinrich, K. Weidmann, and G. Rogers, "Development of a Direct Injected Neat Methanol Engine For Passenger Car Applications," SAE International, Future Transportation Conference and Exposition, August 1990.

[12] V. Aesoy, and H. Valland, "Hot Surface Assisted Compression Ignition of Natural Gas in a Direct Injection Diesel Engine," SAE International Congress and Exposition, February, 1996.

[13] I. M. Gogelov, and J. S. Wallace, "Study of Assisted Compression Ignition in a Direct Injected Natural Gas Engine," *J. Eng. Gas Turbines and Power* 139, 122802-1-12, 2017.

[14] S. X. Cheng and J. S. Wallace, "Modeling of Ignition and Combustion for Glow Plug Assisted Direct Injection Natural Gas Engines," ASME Internal Combustion Engine Division Fall Technical Conference, September 2012.

[15] B. Baird, and S. Etemad, "Advanced Glow Plug for Heavy Fuels Applications," SAE International, SAE World Congress & Exhibition, April 2013.

[16] J. V. Pastor, V. Bermudez, J. M. García-Oliver, and J. G. Ramírez-Hernández, "Influence of spray-glow plug configuration on cold start combustion for high-speed direct injection diesel engines," *Energy* 36, 5486-5496, 2011.

[17] C. J. Mueller, and M. P. Musculus, "Glow Plug Assisted Ignition and Combustion of Methanol in an Optical DI Diesel Engine," SAE International Spring Fuels & Lubricants Meeting & Exhibition, May 2001.

[18] P. Adomeit, M. Jakob, A. Kolbeck, and S. Pischinger, "Glow-plug Ignition of Ethanol Fuels under Diesel Engine Relevant Thermodynamic Conditions," SAE International, SAE World Congress & Exhibition, April 2011.

[19] C. Oprea, F. Wong, H. K. Sharif, T. Troczynski, C. Blair, and A. Welch, "Degradation of Silicon Nitride Glow Plugs in Various Environments Part 3: NGDI Engine," *Int. J. Appl. Ceram. Technol.* 9 (2), 272-279, 2012.

[20] C. Allen, G. Mittal, C. Sung, E. Toulson, and T. Lee, "An aerosol rapid compression machine for studying energetic-nanoparticle-enhanced combustion of liquid fuels," *Proc. Combust. Inst.* 33, 3367-3374, 2011.

[21] C. Allen, E. Toulson, T. Edwards, and T. Lee, "Application of a novel charge preparation approach to testing the autoignition characteristics of JP-8 and camelina hydroprocessed renewable jet fuel in a rapid compression machine," *Combust. Flame* 159 (9), 2780-2788, 2012.

[22] D. Valco, K. Min, A. Oldani, T. Edwards, and T. Lee, "Low temperature autoignition of conventional jet fuels and surrogate jet fuels with targeted properties in a rapid compression machine," *Proc. Combust. Inst.* 36, 3687-3694, 2017.

[23] G. Mittal and C. Sung, "Aerodynamics inside a rapid compression machine," *Combust. Flame* 145, 160-180, 2006.

[24] A. Burcat and B. Ruscic, "Third Millennium Ideal Gas and Condensed Phase Thermochemical Database for Combustion with Updates from Active Thermochemical Tables," Argonne National Laboratory Report, September 2005.

[25] M. Kurman, L. Bravo, and C. Kweon, "The Effect of Fuel Injector Nozzle Configuration on JP-8 Sprays at Diesel Engine Conditions," ILASS Americas, Conference on Liquid Atomization and Spray Systems, May 2014.

[26] M. Fabbroni, and J. S. Wallace, “Ignition by Shielded Glow Plug in Natural Gas Fueled Direct Injection Engines,” ASME Internal Combustion Engine Division Fall Technical Conference, October 2011.

[27] K. Min, D. J. Valco, A. Oldani, K. Kim, J. Temme, C. M. Kweon, and T. Lee, “Autoignition of varied cetane number fuels at low temperatures,” *Proc. Combust. Inst.* 37 (4), 5003-5011, 2019.

[28] K. Kim, K. Min, J. Temme, C. M. Kweon, and T. Lee, “Effects of F-24/ATJ blend composition on ignition kinetics at low temperatures,” AIAA SciTech Forum, January 2020.

[29] K. Miwa, T. Ohmija, and T. Nishitani, “A Study of the Ignition Delay of Diesel Fuel Spray Using a Rapid Compression Machine,” *JSME Int. J.* 31 (1), 166-173, 1988.

[30] S. Kobori, T. Kamimoto, and A. A. Aradi, A study of ignition delay of diesel fuel sprays, *Int. J. Engine Research* 1 (1), 29-39, 2000.

[31] C. M. Allen, E. Toulson, D. L. S. Hung, H. Schock, D. Miller, and T. Lee, “Ignition Characteristics of Diesel and Canola Biodiesel Sprays in the Low-Temperature Combustion Regime,” *Energy & Fuels* 25, 2896-2908, 2011.

[32] J. A. LoRusso and H. A. Cikanek, “Direct Injection Ignition Assisted Alcohol Engine,” SAE International Congress and Exposition, February 1988.

[33] B. G. Richards, “Methanol-Fueled Caterpillar 3406 Engine Experience in On-Highway Trucks,” SAE International Fuels and Lubricants Meeting and Exposition, October 1990.

[34] D. Chown, C. Habbaky, and J. S. Wallace, “An Experimental Investigation of Combustion Chamber Design Parameters for Hot Surface Ignition,” ASME Internal Combustion Engine Division Fall Technical Conference, October 2014.

[35] M. Sjöberg, and J. E. Dec, “Smoothing HCCI Heat-Release Rates Using Partial Fuel Stratification with Two-Stage Ignition Fuels,” SAE International, SAE World Congress, April 2006.

[36] Y. Wu, V. Modica, X. Yu, and F. Grisch, “Experimental Investigation of Laminar Flame Speed Measurement for Kerosene Fuels: Jet A-1, Surrogate Fuel, and Its Pure Components,” *Energy & Fuels* 32, 2332-2343, 2018.

[37] L. M. Pickett, S. Kook, H. Persson, and Ö. Andersson, “Diesel fuel jet lift-off stabilization in the presence of laser-induced plasma ignition,” *Proc. Combust. Inst.* 32, 2793-2800, 2009.

[38] J. B. Heywood, “Internal Combustion Engine Fundamentals,” McGraw-Hill Inc., 1988.

[39] C. Oprea, F. Wong, H. K. Sharif, and T. Troczynski, “Degradation of Silicon Nitride Glow Plugs in Various Environments Part 1: dc Electric Field in Ambient Air,” *Int. J. Appl. Ceram. Technol.* 8 (3), 669-683, 2011.

[40] K. N. Lee, D. S. Fox, and N. P. Bansal, “Rare earth silicate environmental barrier coatings for SiC/SiC composites and Si_3N_4 ceramics,” *J. European Ceram. Soc.* 25, 1705-1715, 2005.

[41] K. Pan, and J. S. Wallace, “Numerical Studies of Glow Plug Shield on Natural Gas Ignition Characteristics in a Compression-Ignition Engine,” *J. Eng. Gas Turbines Power* 139 (9), 092806-1-11, 2017.

APPENDIX: TECHNICAL DRAWINGS

Hot Surface Device Window Mount

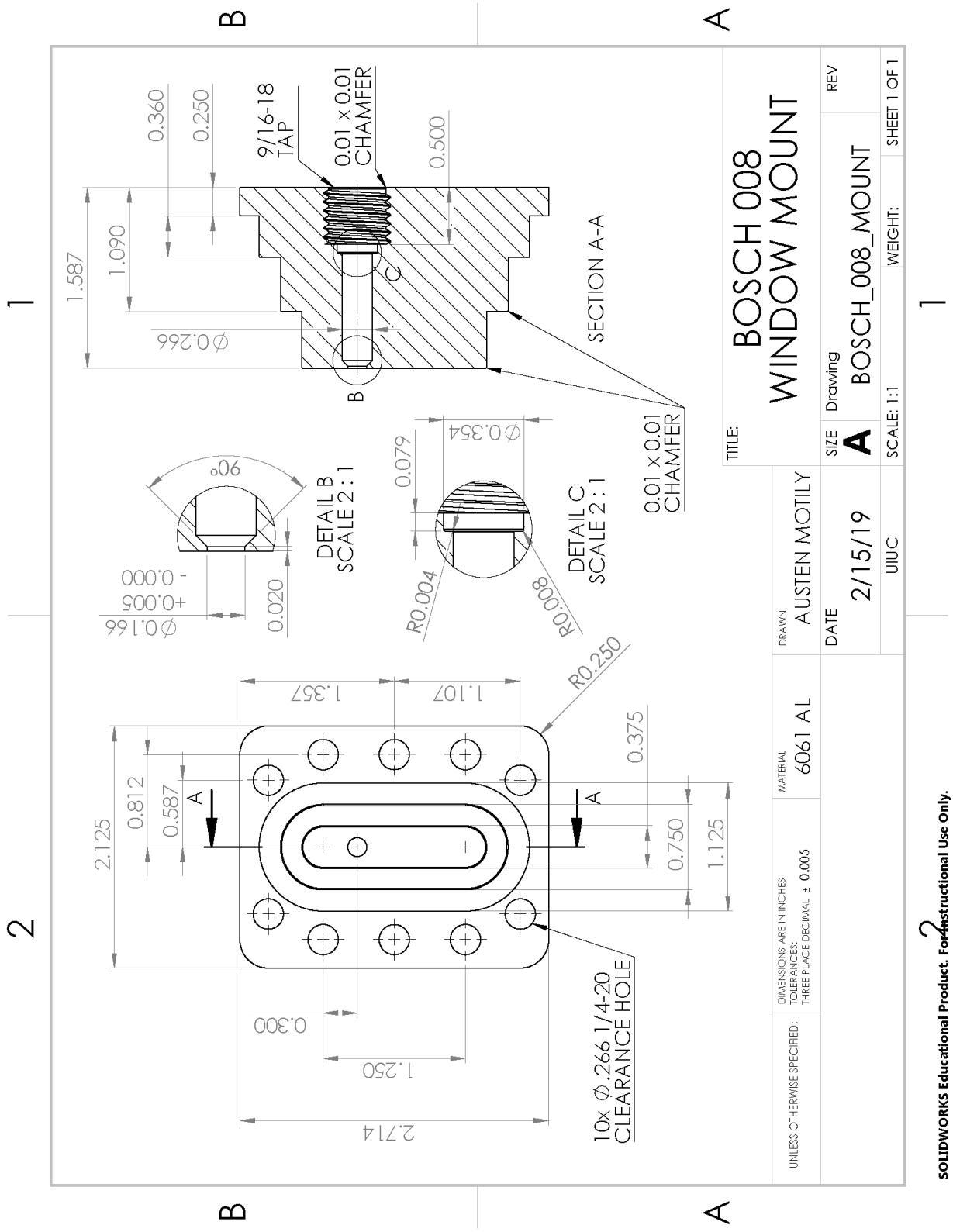

SOLIDWORKS Educational Product. For Instructional Use Only.

Hot Surface Device Mounting Shaft

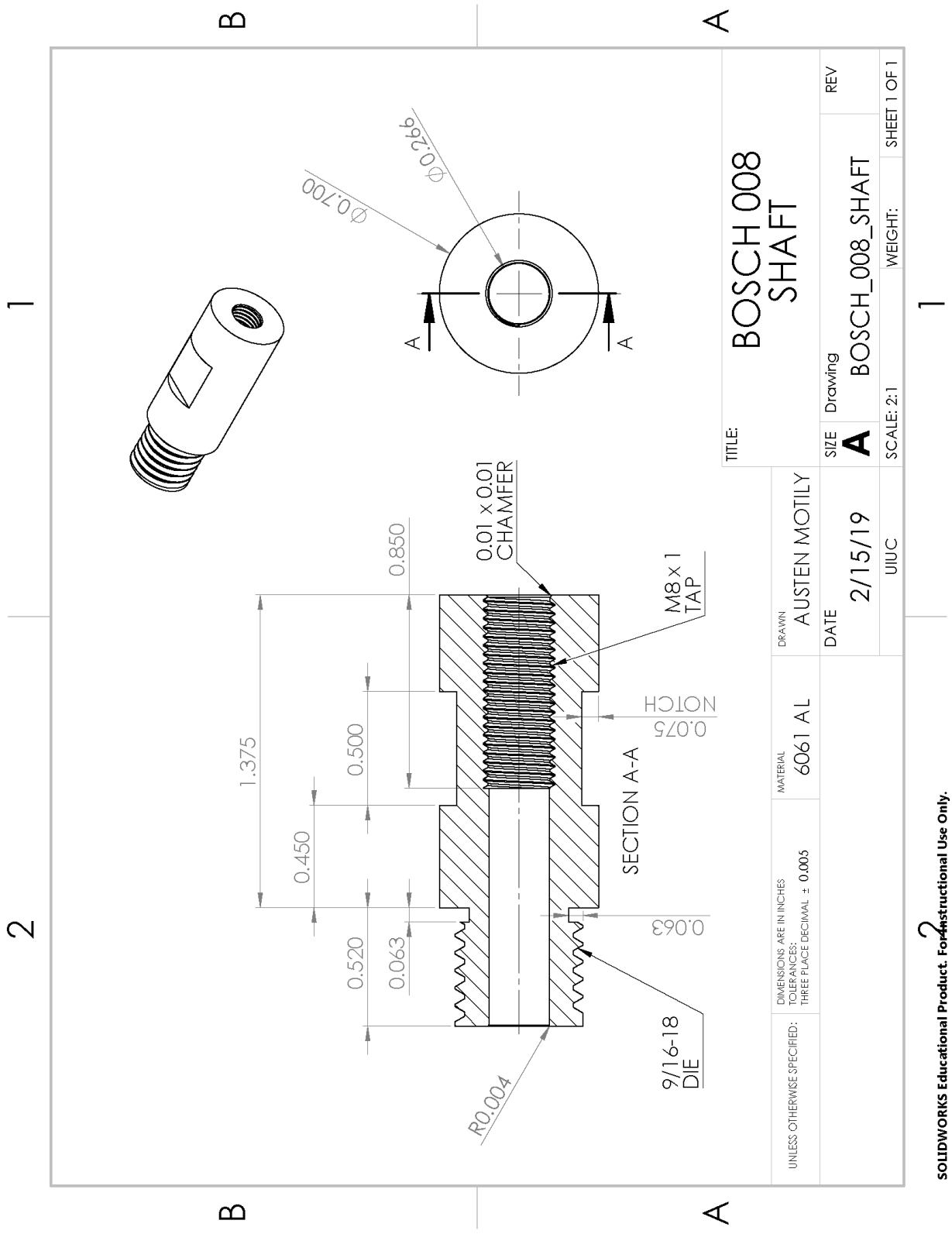

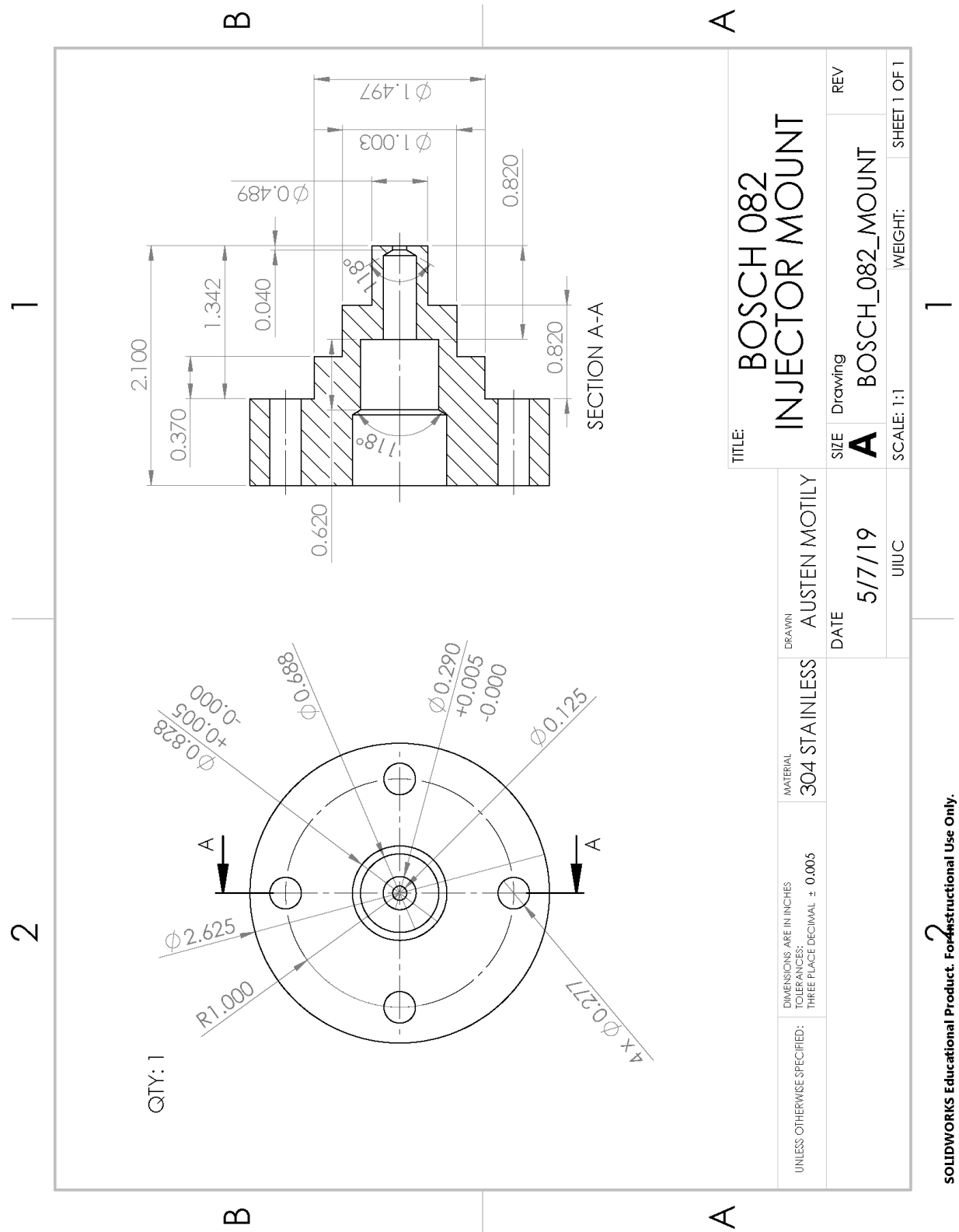
TITLE:
BOSCH 082
INJECTOR MOUNT
SIZE
A
Drawing
BOSCH_082_MOUNT
REV
SCALE: 1:1
WEIGHT:
SHEET 1 OF 1
DRAWN
AUSTEN MOTILY
DATE
5/7/19
UIUC
MATERIAL
304 STAINLESS
DIMENSIONS ARE IN INCHES
TOLERANCES:
THREE PLACE DECIMAL ± 0.005
UNLESS OTHERWISE SPECIFIED:
SECTION A-A
QTY: 1
SOLIDWORKS Educational Product. For Instructional Use Only.

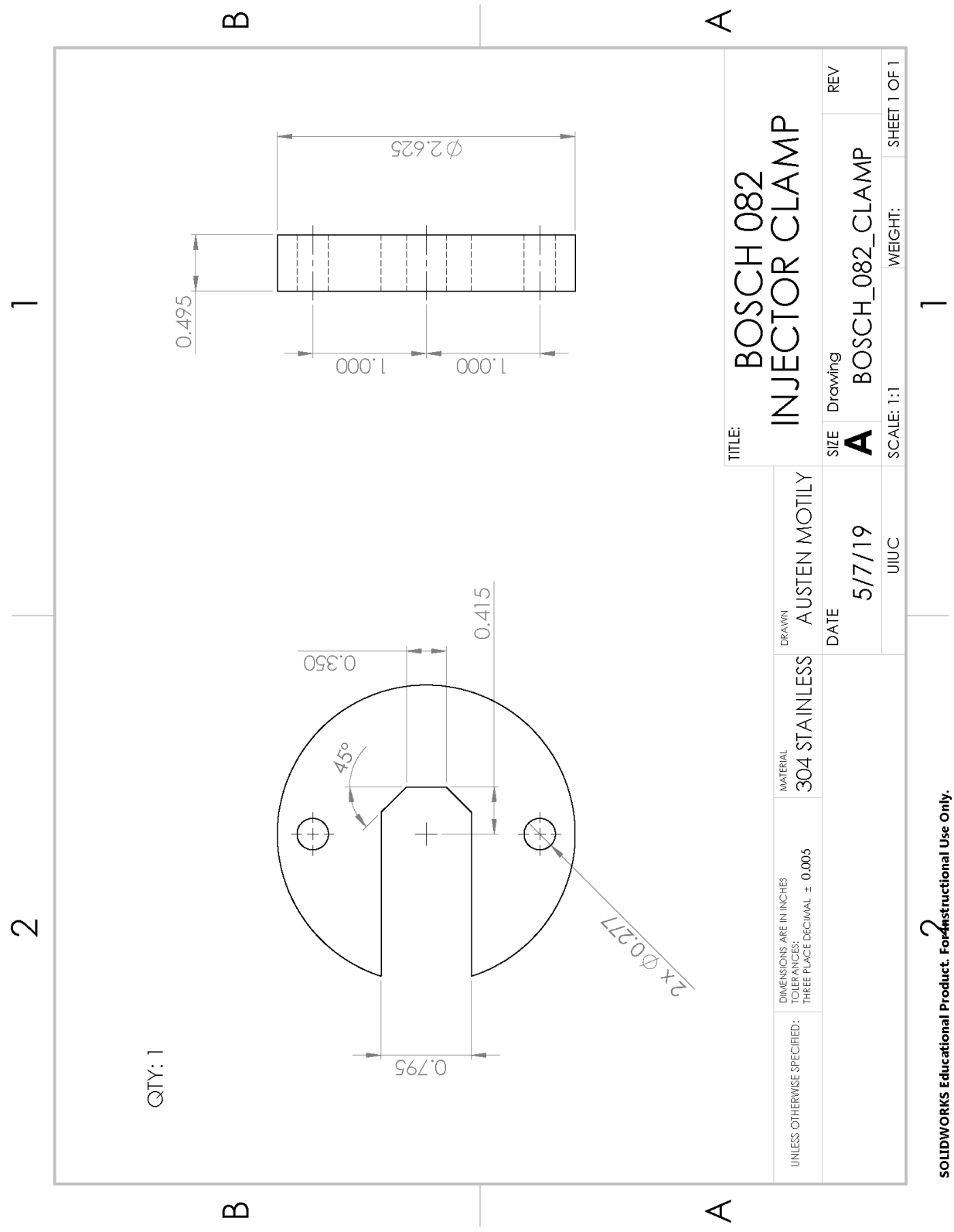
TITLE:
BOSCH 082
INJECTOR CLAMP
SIZE
A
Drawing
BOSCH_082_CLAMP
REV
SCALE: 1:1
WEIGHT:
SHEET 1 OF 1
DRAWN
AUSTEN MOTILY
DATE
5/7/19
UIUC
MATERIAL
304 STAINLESS
DIMENSIONS ARE IN INCHES
TOLERANCES:
THREE PLACE DECIMAL ± 0.005
UNLESS OTHERWISE SPECIFIED:
QTY: 1
0.495
Ø2.625
1.000
1.000
0.350
0.415
45°
0.795
2 x Ø0.277
SOLIDWORKS Educational Product. For Instructional Use Only.